

BROWNIAN MOTION OF A MASSIVE BINARY

DAVID MERRITT

Department of Physics and Astronomy

Draft version November 23, 2018

ABSTRACT

The dynamical friction and diffusion coefficients are derived for a massive binary that moves against a uniform background of stars. The random impulses exerted on the binary’s center of mass by the field stars are greater than those exerted on a point particle due to inelastic scattering. The frictional force acting on the binary is less than that acting on a point particle due to randomization of the trajectories of field stars that pass near the binary. Both effects tend to increase the random motion of a binary compared with that of a point mass. If the maximum effective impact parameter for gravitational encounters is comparable to the radius of gravitational influence of the binary, its Brownian velocity can be increased by a modest factor ($\lesssim 2$) compared with that of a single particle. This condition is probably fulfilled in the case of binary supermassive black holes in galactic nuclei.

1. INTRODUCTION

Brownian motion, the irregular motion exhibited by a heavy particle immersed in a fluid of lighter particles, is usually modelled by the Langevin equation,

$$\frac{d\mathbf{v}}{dt} = -A\mathbf{v} + \mathbf{F}(t). \quad (1)$$

Here \mathbf{v} denotes the velocity of the heavy particle, $-A\mathbf{v}$ is the frictional force from the fluid, and $\mathbf{F}(t)$ is the fluctuating force that arises from collisions between the heavy particle and the fluid particles. The precise form of $\mathbf{F}(t)$ is typically not known but its statistical properties are well defined; for instance, the mean value of \mathbf{F} is zero and its fluctuations generally occur on a time scale that is short compared to the characteristic time over which \mathbf{v} varies. When these conditions are met, the evolution of the single-particle distribution function f is described by the Fokker-Planck equation (e.g. van Kampen 1992); the dynamical friction coefficient that appears in that equation is just A , and the diffusion coefficient is related to the amplitude of \mathbf{F} via the requirement that the steady-state motion be in energy equipartition with the fluid at temperature T (Einstein 1955).

This paper is concerned with the Brownian motion of a massive *binary*, consisting of two point particles whose center of mass moves irregularly due to random gravitational encounters with field stars. The Brownian motion of a binary differs from that of a single particle because the kinetic energy of a field star is not conserved following a close interaction with the binary. If the binary’s mass is much greater than that of a field star, most binary-field star interactions will extract energy from the binary (Heggie 1975), increasing the field star’s kinetic energy and hence the recoil velocity of the binary’s center of mass. This “super-elastic scattering” will give the binary a larger random velocity than expected for a point particle in energy equipartition with background stars, or

$$\langle v^2 \rangle = \frac{m_f}{M} \langle v_f^2 \rangle, \quad (2)$$

where M and m_f are the mass of the heavy particle and of a field star respectively, and $\langle v_f^2 \rangle$ is the mean square velocity of the field stars.

A motivation for the work presented here is the likely existence of binary black holes. There are at least two environments where binary black holes are expected to form. In globular clusters, stars with initial masses exceeding $\sim 20M_\odot$ should comprise $\sim 0.1\%$ by number of the first generation of stars; these massive stars would leave behind black holes with masses $M_\bullet \sim 10M_\odot$, which would rapidly fall to the cluster center and form black-hole binaries (Portegies Zwart & McMillan 1999). Subsequent close encounters will eject most of the black holes, with perhaps a single binary remaining at the cluster center after $\sim 10^9$ yr (Portegies Zwart & McMillan 2000). Binary black holes are also expected to form in galactic nuclei following galaxy mergers (Begelman, Blandford & Rees 1980); here the characteristic masses are $M_\bullet \sim 10^8 M_\odot$. The evolution of a binary supermassive black hole due to encounters with stars has been modelled by Makino (1997), Quinlan & Hernquist (1997) and others using N -body codes. Quinlan & Hernquist (1997) found that the wandering of the binary in their simulations was a factor 5 – 10 greater in amplitude than expected on the basis of equation (2), and attributed this difference to inelastic scattering of stars off the binary.

More speculatively, the massive halos of the Milky Way and other galaxies may contain large numbers of black holes. A population of stellar-mass, primordial black holes has been proposed to explain the gravitational microlensing results toward the Large Magellanic Cloud (Alcock et al. 1997). A small fraction of these black holes would be expected to form binaries through three-body interactions (Nakamura, Sasaki & Tanaka 1997). Alternatively, the halos of galaxies like the Milky Way may consist of black holes of mass $\sim 10^6 M_\odot$ (Carr, Bond & Arnett 1984; Lacey & Ostriker 1985) which would sink toward the galactic center and form binary systems there (Hut & Rees 1992).

The contribution of inelastic scattering to the random motion of a massive binary can be estimated as follows. Define a to be the semi-major axis of the binary and $M_{12} = M_1 + M_2$ its mass, with $M_{12} \gg m_f$. The impact parameter p corresponding to a closest-approach distance r_p of a field star to the binary is

$$p^2 = r_p^2 \left(1 + \frac{2GM_{12}}{V^2 r_p} \right) \approx \frac{2GM_{12}}{V^2} r_p \quad (3)$$

with V the relative velocity at infinity. The rate of encounters with stars that interact strongly with the binary, $r_p \lesssim a$, is then $\sim n_f(\pi p^2)\sigma_f \approx 2\pi n_f GM_{12}a/\sigma_f$ with n_f the number density of field stars. These stars are ejected with typical velocities $v_{ej} \approx \sqrt{GM_{12}/a}$, the binary orbital velocity (Hills & Fullerton 1980), yielding a rate of energy extraction from the binary of

$$\left| \frac{dE_b}{dt} \right| \approx \left(\frac{1}{2} m_f \frac{GM_{12}}{a} \right) \times \left(\frac{2\pi n_f GM_{12}a}{\sigma_f} \right) \approx \frac{\pi G^2 M_{12}^2 \rho_f}{\sigma_f} \quad (4)$$

with $\rho_f = m_f n_f$. We can also write

$$\left| \frac{dE_b}{dt} \right| = \frac{d}{dt} \left(\frac{G(M_{12}/2)^2}{2a} \right) \quad (5)$$

(assuming $M_1 = M_2$), which, together with equation (4), implies the well-known result that a hard binary hardens at a constant rate (Heggie 1975):

$$\frac{d}{dt} \left(\frac{1}{a} \right) \approx \frac{8\pi G \rho_f}{\sigma_f}. \quad (6)$$

The hardening rate is usually expressed in terms of a dimensionless constant H as

$$\frac{d}{dt} \left(\frac{1}{a} \right) \equiv H \frac{G \rho_f}{\sigma_f}. \quad (7)$$

Three-body scattering experiments (Hills 1983; Mikkola & Valtonen 1992; Quinlan 1996) give $H \approx 15$ for a hard ($GM_{12}/a \gg \sigma_f^2$), equal-mass, circular-orbit binary with $M_{12} \gg m_f$.

In terms of H , the energy extraction rate is given precisely by

$$\left| \frac{dE_b}{dt} \right| = \frac{d}{dt} \left(\frac{GM_{12}^2}{8a} \right) = \frac{G^2 M_{12}^2 \rho_f}{8\sigma_f} H. \quad (8)$$

Momentum conservation implies that almost all of the binding energy released during an encounter will go into kinetic energy of the field star. Thus

$$\delta E_b \approx \delta E_* \approx \frac{1}{2} m_f (\delta v_*)^2 \approx \frac{1}{2} m_f \left(\frac{M_{12}}{m_f} \delta v \right)^2 \quad (9)$$

with δv the change in the center-of-mass velocity of the binary; the last relation follows from conservation of momentum. The rate of diffusion in velocity of the binary due to super-elastic scattering is then

$$\langle (\Delta v)^2 \rangle_{S.E.} \approx \frac{2m_f}{M_{12}^2} \left| \frac{dE_b}{dt} \right| \approx \frac{H}{4} \frac{G^2 m_f \rho_f}{\sigma_f}. \quad (10)$$

This diffusion rate may be compared with Chandrasekhar's expression for a point mass initially at rest,

$$\langle (\Delta v)^2 \rangle_C = 8(2\pi)^{1/2} \frac{G^2 m_f \rho_f}{\sigma_f} \ln \Lambda, \quad (11)$$

with $\ln \Lambda \equiv \ln(p_{max}/p_{min})$, the Coulomb logarithm (Spitzer 1987, eq. 2-12). Both diffusion coefficients scale in the same way with the parameters (m_f, ρ_f, σ_f) that define the field star distribution, except for the weak variation implicit in the Coulomb logarithm. The ratio of the two coefficients,

$$\sim \frac{H}{32\sqrt{2\pi} \ln(p_{max}/p_{min})}, \quad (12)$$

therefore depends only on $\ln \Lambda$ and H , reflecting the fact that the Chandrasekhar coefficient is dominated by distant encounters while the effects of super-elastic scattering are limited to close encounters. A more exact definition of $\ln \Lambda$, and appropriate choices for p_{max} and p_{min} , will be presented below; here we note that p_{min} is of order $GM_{12}/\sigma_f^2 \equiv r_G$, the radius of gravitational influence of the massive binary. If the distribution of field stars around the binary falls off steeply over a radius comparable to r_G , p_{max} will be comparable to p_{min} and $\ln \Lambda$ will be small. Equation (12) therefore predicts

that super-elastic scattering will increase the amplitude of the binary's random velocity by a modest amount compared to the random velocity of a point particle with the same mass.

There is a second way in which energy exchange between field stars and the binary will act to increase the magnitude of the binary's random velocity. Brownian motion represents a balance between dynamical friction and scattering. But field stars that interact strongly with the binary are ejected in nearly random directions, and this reduces the dynamical friction force that they exert on the binary. The velocity change experienced by a field star in a low-impact-parameter collision with a point-mass perturber is $\sim -2V$, corresponding to a 180° change in its direction (cf. equation 28). When the point mass is replaced by a hard binary, the field star is ejected in a nearly random direction and its mean velocity change (averaged over many encounters with different phases and orientations of the binary) is therefore $\sim -V$ in a direction parallel to \mathbf{V} . The drag force exerted on the massive object is proportional to the mean velocity change of the field stars and hence the contribution to the frictional force from close encounters is only $\sim 1/2$ as great in the case of a binary as in the case of a point mass.

At first sight, this reduction in the frictional force might appear to be significant. In the standard treatment (e.g. Spitzer 1987, eq. 2-46), dynamical friction arises entirely from field stars with velocities less than that of the massive object. If a massive binary were moving slowly, all of these field stars would have small relative velocities as well and would interact strongly with it. However it turns out (§2.1) that the standard treatment is incorrect in this regard and the reduction in dynamical friction is correspondingly more modest (§4.1).

The approach adopted in the present paper consists of calculating the dynamical friction and diffusion coefficients for a massive binary under exactly the same approximations adopted by Chandrasekhar (1942) in his analysis of gravitational encounters with a point mass. In the case of a binary, this calculation requires the numerical integration of a large number of binary-field star interactions, i.e. scattering experiments (§4). The dynamical friction and diffusion coefficients can then be computed by taking appropriate averages over the velocity changes experienced by the field stars in these experiments. Comparing the coefficients computed for the binary to those computed by Chandrasekhar for a point mass gives the increase in the expected magnitude of the binary's random velocity compared to that of a point mass with $M = M_{12}$. The restriction in the present paper to a massive binary, $M_{12} \gg m_f$, permits a number of simplifications; for instance, the mass of the field star can be neglected in the scattering experiments, and the values of the dynamical friction and diffusion coefficients need only be computed in the limit $v \ll \sigma_f$ appropriate to a massive body that is near energy equipartition with much lighter stars.

It became clear after this investigation was begun that the Chandrasekhar coefficients as they are usually presented could not be directly compared with the results of the scattering experiments. Starting with Chandrasekhar (1943a), the dependence of the Coulomb logarithm on the velocity of the field star has generally been ignored when integrating over the field star velocity distribution (e.g. Rosenbluth, MacDonald & Judd 1957; Hénon 1973). This approximation is valid in the case of a test star whose velocity is comparable to that of the field stars but not when $v \ll \sigma_f$, which is the case of interest here. Thus in §2 the Chandrasekhar coefficients are re-derived without the usual approximations. One of the interesting results of this re-derivation is that the dynamical friction force on a slowly-moving body is found to come primarily from field stars with $v_f > v$. In the standard treatment, all of the frictional force comes from field stars moving more *slowly* than the test star.

An important preliminary step is to relate the equilibrium velocity distribution of a test mass (single star or binary) to its dynamical friction and diffusion coefficients, via the Fokker-Planck equation. This is done in §2. Applications of the results to various physical systems are discussed in §5.

2. FOKKER-PLANCK EQUATION

We wish to compute the equilibrium velocity distribution $f(v)$ of a massive binary that interacts via gravitational encounters with individual stars; \mathbf{v} is the velocity of the binary's center of mass. We assume that the time scale over which this equilibrium is reached is much shorter than the time scale over which the orbital elements of the binary change; this assumption is discussed in more detail in §5.2. We also ignore a possible dependence of f on the direction of \mathbf{v} , appropriate if the orientation of the binary relative to \mathbf{v} is rapidly changing and if the field stars are distributed isotropically in velocity. The dependence of the dynamical friction force on the orientation of the binary is discussed briefly in §4.1. Because of the assumed large mass ratio, $M_{12} \gg m_f$, even close encounters will produce only small deflections in the trajectory of the binary. Hence we may describe the evolution of f via the Fokker-Planck equation (Chandrasekhar 1943b). In a steady state, this equation implies

$$0 = -N(v)\langle\Delta v\rangle + \frac{1}{2}\frac{\partial}{\partial v}[N(v)\langle(\Delta v)^2\rangle] \quad (13)$$

where

$$4\pi v^2 f(v) dv = N(v) dv. \quad (14)$$

The coefficients $\langle\Delta v\rangle$ and $\langle(\Delta v)^2\rangle$ are defined in the usual way as sums, over a unit interval of time, of Δv and $(\Delta v)^2$ due to encounters with field stars.

Define Δv_{\parallel} and Δv_{\perp} to be changes in v in directions parallel and perpendicular to \mathbf{v} . We have

$$\Delta v = \left[(v + \Delta v_{\parallel})^2 + (\Delta v_{\perp})^2 \right]^{1/2} - v. \quad (15)$$

Expanding to second order in the small quantities Δv_{\parallel} and Δv_{\perp} and taking means, the coefficients in equation (13) may be expressed in terms of the usual dynamical friction and diffusion coefficients as

$$\langle \Delta v \rangle = \langle \Delta v_{\parallel} \rangle + \frac{1}{2} \frac{\langle (\Delta v_{\perp})^2 \rangle}{v}, \quad \langle (\Delta v)^2 \rangle = \langle (\Delta v_{\parallel})^2 \rangle. \quad (16)$$

Substituting equations (14) and (16) into equation (13) yields¹

$$0 = f \left[\langle \Delta v_{\parallel} \rangle + \frac{1}{2v} \left(\langle \Delta v_{\perp}^2 \rangle - 2 \langle \Delta v_{\parallel}^2 \rangle \right) \right] - \frac{1}{2} \frac{\partial}{\partial v} \left(f \langle \Delta v_{\parallel}^2 \rangle \right). \quad (17)$$

Equation (17) may also be derived from equation (2-71) of Spitzer (1987) after replacing ∂E in that equation by $v \partial v$ and expressing $\langle \Delta E \rangle$ and $\langle \Delta E^2 \rangle$ in terms of $\langle \Delta v_{\parallel} \rangle$, $\langle \Delta v_{\parallel}^2 \rangle$ and $\langle \Delta v_{\perp}^2 \rangle$.

In a steady state, we expect that v will be of order $\sqrt{m_f/M_{12}} \ll 1$ times the velocity dispersion σ_f of the field stars. Hence it is appropriate to expand the dynamical friction and diffusion coefficients about $v = 0$:

$$\langle \Delta v_{\parallel} \rangle = -Av + Bv^3 \dots, \quad (18a)$$

$$\langle \Delta v_{\parallel}^2 \rangle = C + Dv^2 \dots, \quad (18b)$$

$$\langle \Delta v_{\perp}^2 \rangle = 2(E + Fv^2) \dots \quad (18c)$$

Substituting these expressions into equation (17) gives

$$0 = (-Av^2 + Bv^4 + E + Fv^2 - C - 2Dv^2) f - \frac{v}{2} (C + Dv^2) \frac{\partial f}{\partial v}. \quad (19)$$

Setting $v = 0$ gives $C = E$, i.e. the diffusion rate of a stationary particle must be independent of direction. Cancelling additional terms, we find to lowest order in v

$$0 = (A + 2D - F) f + \frac{C}{2} \frac{\partial f}{\partial v} \frac{1}{v}. \quad (20)$$

The standard Chandrasekhar coefficients for a point particle of mass M interacting with stars of mass m_f (e.g. Spitzer 1987, eqs. 2-52 – 2-54) give, after expanding about $v = 0$:

$$A_C = \frac{4\sqrt{2\pi}}{3} \frac{G^2 m_f^2 n_f \ln \Lambda}{\sigma_f^3} \left(1 + \frac{M}{m_f} \right), \quad B_C = \frac{3}{10} \frac{A_C}{\sigma_f^2}, \quad (21a)$$

$$C_C = \frac{8\sqrt{2\pi}}{3} \frac{G^2 m_f^2 n_f \ln \Lambda}{\sigma_f}, \quad D_C = -\frac{3}{10} \frac{C_C}{\sigma_f^2}, \quad (21b)$$

$$E_C = C_C, \quad F_C = -\frac{1}{10} \frac{C_C}{\sigma_f^2}. \quad (21c)$$

Thus

$$A_C + 2D_C - F_C = A_C - \frac{C_C}{2\sigma_f^2} \quad (22a)$$

$$= -\frac{4\sqrt{2\pi}}{3} \frac{G^2 M m_f n_f \ln \Lambda}{\sigma_f^3} \quad (22b)$$

$$\approx A_C \quad (22c)$$

where the last relation is valid when $M \gg m_f$. In the case of the more general coefficients describing the motion of a massive binary, A will still be of order M_{12}/m_f times D and F and we may likewise approximate $(A + 2D - F)$ by A . Thus

$$0 \approx A f + \frac{C}{2} \frac{\partial f}{\partial v} \frac{1}{v} \quad (23)$$

which has solution

$$f(v) = f_0 e^{-v^2/2\sigma^2}, \quad (24a)$$

$$\sigma^2 = \frac{C}{2A}. \quad (24b)$$

¹ In equation (17) and below, the parentheses in expressions like $\langle (\Delta v_{\parallel})^2 \rangle$ are dropped.

Substituting A_C for A and C_C for C gives the well-known result for the equipartition velocity dispersion of a point mass,

$$\sigma_C = \left(\frac{m_f}{M}\right)^{1/2} \sigma_f. \quad (25)$$

It will be useful in what follows to express the coefficients A and C for a massive binary in terms of their values for a point mass with $M = M_{12}$, i.e. in terms of the ratios

$$R_1 \equiv \frac{A}{A_C}, \quad R_2 \equiv \frac{C}{C_C}. \quad (26)$$

(The Chandrasekhar coefficients A_C and C_C will be defined slightly differently below.) The velocity dispersion of the binary is then

$$\sigma = \left(\frac{R_2}{R_1}\right)^{1/2} \left(\frac{m_f}{M_{12}}\right)^{1/2} \sigma_f. \quad (27)$$

Thus the problem of determining the equilibrium velocity distribution of the binary's center-of-mass motion is reduced to determining the ratios of $\langle \Delta v_{\parallel} \rangle$ and $\langle \Delta v_{\parallel}^2 \rangle$, the dynamical friction and diffusion coefficients for the binary, to the Chandrasekhar coefficients for a point mass in the low- v limit. We note that R_2 can equally well be defined as $(C + 2E)/(C_C + 2E_C)$, i.e. in terms of the diffusion coefficient $\langle \Delta v^2 \rangle = \langle \Delta v_{\parallel}^2 \rangle + \langle \Delta v_{\perp}^2 \rangle$, in the limit $v \rightarrow 0$.

3. CHANDRASEKHAR COEFFICIENTS FOR A POINT MASS

The Chandrasekhar coefficients for a point mass in the form given above (eqs. 21a–21c) embody two approximations: the argument of $\ln \Lambda$ was assumed constant when integrating over the distribution of field-star velocities; and the non-dominant terms, which are of order $1/\ln \Lambda$ or $1/\Lambda$ times the dominant terms, were ignored. Both approximations are reasonable when the velocity of the test star is not too different from the typical velocity of the field stars, and when the integration over impact parameters extends to distances much greater than GM/σ_f^2 . However it is impossible to reproduce these approximations precisely when carrying out the scattering experiments discussed below; hence in order to compute the ratios (eqs. 26) between the coefficients for the binary and for a point mass, we must first rederive the Chandrasekhar coefficients without the usual approximations. Of particular interest here is the velocity dependence of the Coulomb logarithm. Chandrasekhar (1943a) and White (1949) noted that this dependence implies that some of the dynamical friction force comes from field stars moving more rapidly than the test mass; in the standard treatment, where $\ln \Lambda$ is removed from the integral over field star velocities, all of the friction is produced by field stars with $v_f < v$. An exact analysis in the case of interest here, $v \ll \sigma_f$, has apparently never been carried out. We will find in fact that almost all of the frictional force comes from field stars with $v_f > v$ in the low-velocity limit. We also derive a precise expression for the Coulomb logarithm in this limit.

3.1. Dynamical Friction

The velocity change of a test particle of mass M in one encounter with a field particle of mass $m_f \ll M$ is (Spitzer 1987, eq. 2-19)

$$\Delta v_{\parallel} = -2V \frac{m_f}{M} \frac{1}{1 + p^2/p_0^2} \quad (28)$$

where V is the relative velocity at infinity, p is the impact parameter, and $p_0 \equiv GM/V^2$. Multiplying by $2\pi p n_f V dp$, with n_f the number density of field stars, and integrating over p gives

$$\overline{(\Delta v_{\parallel})} = -\frac{2\pi G^2 M m_f n_f}{V^2} \ln(1 + p_{\max}^2/p_0^2), \quad (29)$$

the rate of change of v_{\parallel} due to encounters with field stars of velocity V .

The dynamical friction coefficient is (Spitzer 1987, eq. 2-28)

$$\langle \Delta v_{\parallel} \rangle = \int f_f(\mathbf{v}_f) \overline{(\Delta v_{\parallel})} \frac{v - v_{fx}}{V} d\mathbf{v}_f \quad (30a)$$

$$= -2\pi G^2 M m_f n_f \int f_f(\mathbf{v}_f) \frac{v - v_{fx}}{V^3} \ln\left(1 + \frac{p_{\max}^2 V^4}{G^2 M^2}\right) d\mathbf{v}_f, \quad (30b)$$

with v the velocity of the (massive) test particle, f_f the distribution of field-star velocities (normalized to unit total number) and $\mathbf{V} = \mathbf{v} - \mathbf{v}_f$; \mathbf{v} has been assumed parallel to the x -axis. Following Chandrasekhar (1943a), we can represent the velocity-space volume element in terms of v_f and V ; then writing

$$v - v_{fx} = \frac{V^2 + v^2 - v_f^2}{2v} \quad (31)$$

gives

$$\langle \Delta v_{\parallel} \rangle = -2\pi^2 G^2 M m_f n_f v^{-2} \int_0^{\infty} dv_f v_f f_f(v_f) \int_{|v-v_f|}^{v+v_f} dV \left(1 + \frac{v^2 - v_f^2}{V^2} \right) \ln \left(1 + \frac{p_{max}^2 V^4}{G^2 M^2} \right) \quad (32)$$

where f_f is henceforth assumed isotropic.

In the standard approximation (e.g. Rosenbluth, MacDonald & Judd 1957), the velocity dependence of the logarithmic term is ignored, and one writes

$$\ln \left(1 + \frac{p_{max}^2 V^4}{G^2 M^2} \right) \approx 2 \ln \Lambda, \quad \Lambda \equiv \frac{p_{max}}{p_{min}}. \quad (33)$$

The dynamical friction coefficient then becomes

$$\langle \Delta v_{\parallel} \rangle = -4\pi(4\pi G^2 M m_f n_f) \int_0^{\infty} dv_f \left(\frac{v_f}{v} \right)^2 f_f(v_f) H_1(v, v_f, p_{max}) \quad (34)$$

with

$$H_1 = \begin{cases} \ln \Lambda & \text{if } v > v_f, \\ 0 & \text{if } v < v_f. \end{cases} \quad (35)$$

Neither p_{max} nor p_{min} are well-defined; p_{min} is typically set to some multiple of GM/σ_f^2 (e.g. Spitzer 1987, eq. 2-14). Equation (35) reproduces the well-known result that only field stars with $v_f < v$ contribute to the frictional force.

When the velocity of the test particle is sufficiently low, as in the case of a massive particle near equipartition with lighter field particles, the logarithm in equation (32) will be close to zero for *all* stars with $v_f < v$. Hence it is unclear whether removing the logarithm from the integrand is a reasonable approximation, or what the proper definition of $\ln \Lambda$ (particularly p_{min}) in the final expression should be. The frictional force in the low- v limit must either be much less than implied by equation (34), or else most of the frictional force must come from field stars with $v_f > v$.

In fact the latter is the case, as we now show. Returning the logarithmic term to the integrand in equation (34) gives

$$H_1(v, v_f, p_{max}) = \frac{1}{8v_f} \int_{|v-v_f|}^{v+v_f} dV \left(1 + \frac{v^2 - v_f^2}{V^2} \right) \ln \left(1 + \frac{p_{max}^2 V^4}{G^2 M^2} \right). \quad (36)$$

This function is plotted in Figure 1a. For low test-star velocities, $v \lesssim \sqrt{GM/p_{max}}$, H_1 deviates strongly from a step function; it reaches a peak at $v_f \approx \sqrt{GM/p_{max}}$ and its peak amplitude varies as $\sim v^3$ due to the velocity dependence of the logarithm. Figure 1b plots the (normalized) integrand of the dynamical friction integral, equation (34), in the limits of low and high v/σ_f . The field-star velocity distribution was assumed to be a Maxwellian:

$$f_f(v_f) = \frac{1}{(2\pi\sigma_f^2)^{3/2}} e^{-v_f^2/2\sigma_f^2}. \quad (37)$$

For low v/σ_f , the integrand of equation (34) may be shown to vary approximately as

$$\frac{x_f^3 e^{-x_f^2/2}}{1 + R^2 x_f^4} \quad (38)$$

where

$$x_f \equiv \frac{v_f}{\sigma_f}, \quad R \equiv \frac{p_{max}}{p_f}, \quad p_f \equiv \frac{GM}{\sigma_f^2}. \quad (39)$$

This function peaks at $x_f \approx R^{-1/2}$. In the case of high v/σ_f , on the other hand, the integrand varies as

$$x_f^2 e^{-x_f^2/2} \quad (40)$$

which peaks at $x_f = 1$. Thus for $R \equiv p_{max}/p_f \approx 1$, the dynamical friction force comes from field stars with $v_f \sim \sigma_f$, whether the test star is moving much faster or much slower than the typical field star! For $R \gtrsim 1$, the frictional force in the low- v limit comes from field stars with $v_f \lesssim \sigma_f/R^{1/2}$; thus for any $v \lesssim \sigma_f/R^{1/2}$, i.e. for $M \gtrsim Rm_f$, most of the stars producing the frictional force will be moving faster than the test star. The appropriate choice for R is discussed in §5 where it is argued that $R \gtrsim 1$ in many cases of interest.

The complete expression for the dynamical friction coefficient is

$$\langle \Delta v_{\parallel} \rangle = -16\sqrt{\pi} G m_f p_f n_f F(v/\sigma_f, p_{max}/p_f), \quad (41a)$$

$$F(x, R) = x^{-2} \int_0^{\infty} dy y^2 e^{-y^2} H_1(x, \sqrt{2}y, R), \quad (41b)$$

$$H_1(x, z, R) = \frac{1}{8z} \int_{|x-z|}^{x+z} dw \left(1 + \frac{x^2 - z^2}{w^2} \right) \ln(1 + R^2 w^4) \quad (41c)$$

where $x \equiv v/\sigma_f$ and R and p_f are defined above. The function $F(v, p_{max})$ is plotted in Figure 2. The dependence of $\langle \Delta v_{\parallel} \rangle$ on v is seen to be a function of R . By contrast, when $\ln \Lambda$ is assumed fixed, the v -dependence of $\langle \Delta v_{\parallel} \rangle$ is independent of p_{max}/p_{min} (Spitzer 1987, eq. 2-52; Fig. 2).

The low- v limit of the frictional force may be derived by careful manipulation of equations (41a - 41c). A more transparent route, useful in what follows, is to first change variables in equation (30a).² Representing the velocity-space volume element in terms of V and λ , where λ is the direction cosine between \mathbf{V} and \mathbf{v}

$$\lambda = \frac{(v\hat{\mathbf{e}}_x - \mathbf{v}_f) \cdot v\hat{\mathbf{e}}_x}{Vv} = \frac{v - v_{f,x}}{V}, \quad (42)$$

gives

$$\langle \Delta v_{\parallel} \rangle = -2\pi G^2 M m_f n_f \times 2\pi \int_0^\infty dV V^2 \int_{-1}^1 d\lambda \frac{\lambda}{V^2} f_f(v_f) \ln \left(1 + \frac{p_{max}^2 V^4}{G^2 M^2} \right) \quad (43a)$$

$$= -4\pi^2 G^2 M m_f n_f \int_0^\infty dV \ln \left(1 + \frac{p_{max}^2 V^4}{G^2 M^2} \right) \int_{-1}^1 d\lambda \lambda f_f(v_f). \quad (43b)$$

Again substituting equation (37) for f_f and integrating over λ ,

$$\begin{aligned} \langle \Delta v_{\parallel} \rangle &= -\frac{2\sqrt{2\pi} G^2 M m_f n_f}{\sigma_f^3} e^{-v^2/2\sigma_f^2} \int_0^\infty dV e^{-V^2/2\sigma_f^2} \ln \left(1 + \frac{p^2 V^4}{G^2 M^2} \right) \\ &\times \frac{\sigma_f^4}{v^2 V^2} \left[\frac{vV}{\sigma_f^2} \cosh \left(\frac{vV}{\sigma_f^2} \right) - \sinh \left(\frac{vV}{\sigma_f^2} \right) \right]. \end{aligned} \quad (44)$$

Taking the limit $v \ll \sigma_f$, and writing by analogy with equation (18a)

$$\langle \Delta v_{\parallel} \rangle = -A_C v + B_C v^3 \dots, \quad (45)$$

we find

$$A_C = \frac{2\sqrt{2\pi}}{3} \frac{G^2 M m_f n_f}{\sigma_f^3} \int_0^\infty dz e^{-z} \ln(1 + 4R^2 z^2), \quad (46a)$$

$$B_C = \frac{\sqrt{2\pi}}{15} \frac{G^2 M m_f n_f}{\sigma_f^5} \int_0^\infty dz e^{-z} (5 - 2z) \ln(1 + 4R^2 z^2). \quad (46b)$$

Thus Hooke's law ($\langle \Delta v_{\parallel} \rangle \propto -v$) is recovered for $v \ll \sigma_f$.

Of primary interest here is the leading coefficient, which may be written

$$A_C = \frac{4\sqrt{2\pi}}{3} \frac{G^2 M m_f n_f}{\sigma_f^3} G(R), \quad (47a)$$

$$G(R) \equiv \frac{1}{2} \int_0^\infty dz e^{-z} \ln(1 + 4R^2 z^2). \quad (47b)$$

A reasonable approximation to $G(R)$, valid for $R \gtrsim 1$, is

$$G(R) \approx \ln \sqrt{1 + 2R^2} \approx \ln \sqrt{1 + \frac{2p_{max}^2 \sigma_f^4}{G^2 M^2}} \quad (48)$$

(Figure 3). Comparing equations (47a) and (48) with the standard dynamical friction coefficient for a point mass in the low-test-particle-velocity limit, equation (21a), we find

$$\ln \Lambda \equiv \ln \sqrt{1 + \frac{p_{max}^2}{p_{min}^2}} \approx \ln \sqrt{1 + 2R^2} = \ln \sqrt{1 + \frac{2p_{max}^2 \sigma_f^4}{G^2 M^2}} \quad (49)$$

or

$$p_{min} \approx \frac{GM}{\sqrt{2}\sigma_f^2}. \quad (50)$$

²I am grateful to M. Milosavljević for pointing this out.

Spitzer (1987, eq. 2-14) advocates

$$p_{min} \approx \frac{G(m_f + M)}{6\sigma_f^2} \quad (51)$$

in the case that the test and field stars have similar masses and velocities. When $M \gg m_f$, the denominator in Spitzer's expression should be reduced by a factor ~ 2 to account for the lower relative velocities, giving a value for p_{min} that is not too different from the value derived here. This agreement is not fortuitous: it is a result of the fact that the field stars responsible for producing the frictional force have roughly the same velocity distribution whether the test star is moving rapidly or slowly.

3.2. Diffusion

The squared velocity changes of the test particle in one encounter with a field star are (cf. Spitzer 1987, equations 2-18 and 2-19):

$$(\Delta v_{\parallel})^2 = 4V^2 \frac{m_f^2}{M^2} \frac{1}{(1 + p^2/p_0^2)^2}, \quad (\Delta v_{\perp})^2 = 4V^2 \frac{m_f^2}{M^2} \frac{p^2/p_0^2}{(1 + p^2/p_0^2)^2}. \quad (52)$$

Multiplying by $2\pi p n_f V dp$ and integrating over p as before,

$$\overline{(\Delta v_{\parallel})^2} = \frac{4\pi G^2 n_f m_f^2}{V} \left(\frac{p_{max}^2/p_0^2}{1 + p_{max}^2/p_0^2} \right), \quad (53a)$$

$$\overline{(\Delta v_{\perp})^2} = \frac{4\pi G^2 n_f m_f^2}{V} \left[\ln \left(1 + \frac{p_{max}^2}{p_0^2} \right) - \frac{p_{max}^2/p_0^2}{1 + p_{max}^2/p_0^2} \right], \quad (53b)$$

the rates of change due to encounters with field stars whose velocity at infinity is V .

The expressions just given refer to velocity changes with respect to the direction of the initial relative velocity vector \mathbf{V} . We need to transform to a frame in which the test particle has velocity \mathbf{v} . Following Spitzer (1987, eqs. 2-24, 2-25), but retaining the contributions from the non-dominant terms, gives in the fixed frame

$$\langle \Delta v_i \Delta v_j \rangle = (\hat{\mathbf{e}}_i \cdot \hat{\mathbf{e}}'_1)(\hat{\mathbf{e}}_j \cdot \hat{\mathbf{e}}'_1) \overline{(\Delta v_{\parallel})^2} + \frac{1}{2} [(\hat{\mathbf{e}}_i \cdot \hat{\mathbf{e}}'_2)(\hat{\mathbf{e}}_j \cdot \hat{\mathbf{e}}'_2) + (\hat{\mathbf{e}}_i \cdot \hat{\mathbf{e}}'_3)(\hat{\mathbf{e}}_j \cdot \hat{\mathbf{e}}'_3)] \overline{(\Delta v_{\perp})^2} \quad (54a)$$

$$= \frac{V_i V_j}{V^2} \left[\overline{(\Delta v_{\parallel})^2} - \frac{1}{2} \overline{(\Delta v_{\perp})^2} \right] + \frac{1}{2} \delta_{ij} \overline{(\Delta v_{\perp})^2} \quad (54b)$$

or

$$\langle \Delta v_1 \Delta v_1 \rangle = \frac{V_x^2}{V^2} \overline{(\Delta v_{\parallel})^2} + \frac{1}{2} \left(1 - \frac{V_x^2}{V^2} \right) \overline{(\Delta v_{\perp})^2}, \quad (55a)$$

$$\langle \Delta v_2 \Delta v_2 \rangle + \langle \Delta v_3 \Delta v_3 \rangle = \frac{V_y^2 + V_z^2}{V^2} \overline{(\Delta v_{\parallel})^2} + \left(1 - \frac{1}{2} \frac{V_y^2 + V_z^2}{V^2} \right) \overline{(\Delta v_{\perp})^2} \quad (55b)$$

where the \mathbf{e}_1 axis is oriented parallel to \mathbf{v} . The final integrations over field-star velocities are then

$$\langle \Delta v_{\parallel}^2 \rangle = \frac{2\pi}{v} \int_0^\infty dv_f v_f f_f(\mathbf{v}_f) \int_{|v-v_f|}^{v+v_f} dV V \langle \Delta v_1 \Delta v_1 \rangle, \quad (56a)$$

$$\langle \Delta v_{\perp}^2 \rangle = \frac{2\pi}{v} \int_0^\infty dv_f v_f f_f(\mathbf{v}_f) \int_{|v-v_f|}^{v+v_f} dV V [\langle \Delta v_2 \Delta v_2 \rangle + \langle \Delta v_3 \Delta v_3 \rangle]. \quad (56b)$$

Writing

$$V_x = \frac{V^2 + v^2 - v_f^2}{2v}, \quad V_y^2 + V_z^2 = 1 - V_x^2, \quad (57)$$

we find as before

$$\langle \Delta v_{\parallel}^2 \rangle = \frac{8\pi}{3} (4\pi G^2 m_f^2 n_f) v \int_0^\infty dv_f \left(\frac{v_f}{v} \right)^2 f_f(v_f) H_2(v, v_f, p_{max}), \quad (58a)$$

$$\langle \Delta v_{\perp}^2 \rangle = \frac{8\pi}{3} (4\pi G^2 m_f^2 n_f) v \int_0^\infty dv_f \left(\frac{v_f}{v} \right)^2 f_f(v_f) H_3(v, v_f, p_{max}), \quad (58b)$$

$$H_2(v, v_f, p_{max}) = \frac{3}{8v_f} \int_{|v-v_f|}^{v+v_f} dV \left[1 - \frac{V^2}{4v^2} \left(1 + \frac{v^2 - v_f^2}{V^2} \right)^2 \right] \ln \left(1 + \frac{p_{max}^2 V^4}{G^2 M^2} \right) \quad (58c)$$

$$\begin{aligned}
& + \left[\frac{3}{4} \frac{V^2}{v^2} \left(1 + \frac{v^2 - v_f^2}{v^2} \right) - 1 \right] \frac{p_{max}^2 V^4 / G^2 M^2}{1 + p_{max}^2 V^4 / G^2 M^2}, \\
H_3(v, v_f, p_{max}) &= \frac{3}{8v_f} \int_{|v-v_f|}^{v+v_f} dV \left[1 + \frac{V^2}{4v^2} \left(1 + \frac{v^2 - v_f^2}{V^2} \right)^2 \right] \ln \left(1 + \frac{p_{max}^2 V^4}{G^2 M^2} \right) \\
& + \left[1 - \frac{3}{4} \frac{V^2}{v^2} \left(1 + \frac{v^2 - v_f^2}{v^2} \right) \right] \frac{p_{max}^2 V^4 / G^2 M^2}{1 + p_{max}^2 V^4 / G^2 M^2}.
\end{aligned} \tag{58d}$$

In the standard approximation, $\ln \Lambda$ is assumed to be a constant and the non-dominant terms are ignored, yielding

$$H_2 = \begin{cases} \ln \Lambda \left(\frac{v_f}{v} \right)^2 & \text{if } v > v_f, \\ \ln \Lambda \left(\frac{v}{v_f} \right) & \text{if } v < v_f. \end{cases} \tag{59}$$

$$H_3 = \begin{cases} \ln \Lambda \left(3 - \frac{v_f^2}{v^2} \right) & \text{if } v > v_f, \\ 2 \ln \Lambda \left(\frac{v}{v_f} \right) & \text{if } v < v_f. \end{cases} \tag{60}$$

We are again primarily interested in the low- v limits. Returning to equations (56a) and (56b), expressing the integral in the same (V, λ) variables as in §3.1, and expanding to second order in v/σ_f gives

$$\langle \Delta v_{\parallel}^2 \rangle = C_C + D_C v^2 \dots, \tag{61a}$$

$$\langle \Delta v_{\perp}^2 \rangle = 2(E_C + F_C v^2) \dots, \tag{61b}$$

$$C_C = \frac{8}{3} \sqrt{2\pi} \frac{G^2 m_f^2 n_f}{\sigma_f} \int_0^\infty dz e^{-z} \ln(1 + 4R^2 z^2), \tag{62a}$$

$$D_C = -\frac{2}{15} \sqrt{2\pi} \frac{G^2 m_f^2 n_f}{\sigma_f^3} \int_0^\infty dz e^{-z} (5 + 2z - 2z^2) \ln(1 + 4R^2 z^2), \tag{62b}$$

$$E_C = C_C, \tag{62c}$$

$$F_C = -\frac{2}{15} \sqrt{2\pi} \frac{G^2 m_f^2 n_f}{\sigma_f^3} \int_0^\infty dz e^{-z} (5 - 6z + z^2) \ln(1 + 4R^2 z^2). \tag{62d}$$

The leading terms are

$$C_C = E_C = \frac{8\sqrt{2\pi}}{3} \frac{G^2 m_f^2 n_f}{\sigma_f} G(R), \tag{63}$$

with $G(R)$ again given by equation (47b). Comparing equation (63) with equation (47a), we see that the ratios between the three diffusion coefficients at low v are exactly the same as in the standard treatment with $\ln \Lambda$ assumed constant. Thus we predict the same equilibrium velocity dispersion for a point mass as in equation (25), $\sigma^2 = C_C / 2A_C = (m_f / M) \sigma_f^2$.

In what follows, the expressions (47a) and (63) will be used to define A_C and C_C when computing the ratios R_1 and R_2 of the dynamical friction and diffusion coefficients of the binary to those of a point mass (eqs. 26).

4. SCATTERING EXPERIMENTS

The dynamical friction and diffusion coefficients for a massive binary were computed by carrying out a large number of scattering experiments, in the manner of Hills (1983) and Quinlan (1996). In the limit of large mass ratio M_{12}/m_f , the field star may be treated as a massless particle moving in the potential of the two black holes (Mikkola & Valtonen 1992), which follow unperturbed Keplerian trajectories about their fixed center of mass with semimajor axis a . From the changes in the field star's velocity during the encounter we can infer the corresponding changes in the binary's center-of-mass motion. Let the initial velocity of the field particle be $\mathbf{v}_{f0} = v_{f0} \mathbf{e}_x$ and its final velocity $(v'_{fx} \mathbf{e}_x + v'_{fy} \mathbf{e}_y + v'_{fz} \mathbf{e}_z)$. The velocity changes $(\delta v_x, \delta v_y, \delta v_z)$ of the binary's center of mass following a single collision are

$$\delta v_x = -\frac{m_f}{M_{12}} (v'_{fx} - v_{f0}) = -\frac{m_f}{M_{12}} \delta v_{fx}, \tag{64a}$$

$$\delta v_y = -\frac{m_f}{M_{12}} v'_{fy} = -\frac{m_f}{M_{12}} \delta v_{fy}, \tag{64b}$$

$$\delta v_z = -\frac{m_f}{M_{12}} v'_{fz} = -\frac{m_f}{M_{12}} \delta v_{fz}. \tag{64c}$$

The dynamical friction and diffusion coefficients for the binary are obtained by taking the appropriate averages, over an ensemble of trajectories, of the δv_i 's and their squares, as discussed in more detail below.

Orbits were integrated using the routine DOP853 of Hairer, Nørsett & Wanner (1991), an 8(6)th order embedded Runge-Kutta integrator. The routine automatically adjusts the integration time step to keep the fractional error per step below some level TOL , which was set to 10^{-9} . The forces from the black holes were not softened. Each field star was assumed to begin at a position $(x, y, z) = (\infty, p, 0)$ and was advanced from $r = \infty$ to $r = 50a$ along a Keplerian orbit about a point mass M_{12} . The integrations were terminated when the star had moved a distance from the binary that was at least 100 times its initial distance with positive energy, or when the number of integration steps exceeded 10^6 . The latter condition was met only for the integrations with the lowest initial velocities, and even then, for much fewer than 1% of the integrations. These stars were on orbits that were weakly bound to the binary and that needed to make many revolutions before being expelled. The incomplete integrations were not included when computing the diffusion coefficients below.

The binary was given unit total mass, $M_1 = M_2 = 1/2$ and its center of mass was fixed at the origin. The binary's orbit was assumed to be circular in all of the integrations described below. The orientation of the binary's orbital plane, and its initial phase, were chosen randomly for each integration. The angle ξ between the normal to the binary orbital plane and the initial relative velocity was stored for later use, since velocity changes in the field star are expected to depend systematically on ξ . However most of the results presented below are based on averages over ξ and over the phase of the binary, appropriate if the orientation of the binary relative to \mathbf{v} is changing rapidly due to encounters.

Initial velocities for the scattering experiments were assigned one of the discrete values $K \times V_{\text{bin}} = K \times \sqrt{GM_{12}/a}$ with $K = (0.01, 0.02, 0.03, 0.05, 0.1, 0.2, 0.3, 0.5, 1, 2, 3, 5, 10)$. 10^6 orbits were integrated for each value of K , for a total of 1.3×10^7 integrations. The impact parameters p for each V were chosen from one of 20 intervals corresponding to ranges in scaled pericenter distance r_p/a of $[0, 0.001]$, $[0.001, 0.003]$, $[0.003, 0.01]$, $[0.01, 0.02]$, $[0.02, 0.03]$, $[0.03, 0.05]$, $[0.05, 0.1]$, $[0.1, 0.2]$, $[0.2, 0.3]$, $[0.3, 0.5]$, $[0.5, 1]$, $[1, 2]$, $[2, 3]$, $[3, 5]$, $[5, 10]$, $[10, 20]$, $[20, 30]$, $[30, 50]$, $[50, 100]$ and $[100, 200]$. Impact parameters were chosen randomly and uniformly in p^2 within each interval. Unless otherwise indicated, distances and velocities given below are in program units of a and $(GM_{12}/a)^{1/2}$ respectively.

A number of checks of the numerical integrations were carried out. The field-star velocity changes were used to recompute the binary hardening rates calculated by Mikkola & Valtonen (1992), Hills (1983, 1992) and Quinlan (1996). The agreement was excellent. The relation:

$$H_1(V) = \frac{4v}{G^2 M^2 n_f} \left[2V \overline{(\Delta v_{\parallel})} + \left(\overline{(\Delta v_{\parallel})^2} + \overline{(\Delta v_{\perp})^2} \right) \right], \quad (65)$$

was also checked; here H_1 is the velocity-dependent hardening rate defined by Quinlan (1996), and the diffusion coefficients on the right hand side refer to the field stars. A weaker check (since it does not depend on the details of binary-field star interactions) consisted of verifying that the diffusion coefficients $\langle \Delta v_{\parallel} \rangle$ and $\langle \Delta v_{\perp}^2 \rangle$ for the binary tended to those of a point mass for large p_{max} .

4.1. Dynamical Friction

For a binary initially at rest, the acceleration of its center of mass due to encounters with field stars of initial velocity V is

$$\langle \delta v_x(V, p_{\text{max}}) \rangle = 2\pi n_f V \int_0^{p_{\text{max}}} dp p \overline{\delta v_x}(V, p) = -2\pi n_f \left(\frac{m_f}{M_{12}} \right) V \int_0^{p_{\text{max}}} dp p \overline{\delta v_{fx}}(V, p) \quad (66)$$

where $\overline{\delta v_{fx}}(V, p)$ is the mean change in the x -component of the field star velocity, averaged over many encounters with the binary at fixed (V, p) . We are interested in the ratio between the numerically-computed coefficients and the exact expression for a point mass (equation 29). This ratio is

$$D_1(V, p_{\text{max}}) = -\frac{V^3}{\ln(1 + p_{\text{max}}^2/p_0^2) G^2 M_{12}^2} \int_0^{p_{\text{max}}} dp p \overline{\delta v_{fx}} \quad (67a)$$

$$= -\frac{1}{2 \ln(1 + p_{\text{max}}^2/p_0^2)} \left(\frac{V}{V_{\text{bin}}} \right)^3 \int_0^{p_{\text{max}}/a} d \left(\frac{p}{a} \right)^2 \left(\frac{\overline{\delta v_x}}{V_{\text{bin}}} \right) \quad (67b)$$

with $V_{\text{bin}}^2 \equiv GM_{12}/a$ and $p_0 \equiv GM_{12}/V^2$.

Figure 4 shows values of D_1 , averaged over all orientations of the binary, for several values of V . Generally $D_1 < 1$ due to randomization by the binary of the velocities of test stars that pass within a distance $r_p \lesssim a$. However there is a complicated dependence of D_1 on p_{max} and V . For $V \gg V_{\text{bin}}$, collisions at small impact parameter ($p < a$) result in the field star passing through the binary with almost no change in velocity on average, and hence $D_1 \rightarrow 0$. As V is decreased, the velocity changes in the field star become greater on average and D_1 is determined by the distribution of angles over which field stars are ejected from the binary. Figure 5 shows the distribution of field star velocity changes as a function of p for $V = 0.5V_{\text{bin}}$. At large impact parameters, $p \gg p_{\text{crit}}$, where

$$\frac{p_{\text{crit}}}{a} \approx \sqrt{\frac{2GM_{12}}{V^2 a}}, \quad (68)$$

the velocity changes are distributed in the way expected for interaction with a point mass (Fig. 5a; eq. 28). When $p \approx p_{crit}$, the distribution of δv_f 's broadens due to the change in velocity (both magnitude and direction) resulting from interaction with the binary; the broadened distributions extend to positive δv_f 's, corresponding to stars which are ejected with high velocity in the same direction as their initial motion – producing an “anti-frictional” force on the binary (Fig. 5c). At still smaller impact parameters, $p < p_{crit}$, stars are ejected with a typical angle $\sim \pi/3$ with respect to their initial velocity vector, compared to $\sim \pi$ for interactions with a point mass; thus $|\overline{\delta v_{fx}}|$ is reduced and with it the contribution to the frictional force (Fig. 5d).

The dynamical friction coefficient for the binary is (cf. equation 30a)

$$\langle \Delta v_{\parallel} \rangle = \int f_f(\mathbf{v}_f) \left(\frac{v - v_{fx}}{V} \right) \langle \delta v_x \rangle d\mathbf{v}_f. \quad (69)$$

We are primarily interested in the low- v limit. Repeating the analysis leading to equation (47a) we find, for a Maxwellian f_f ,

$$A = \frac{1}{3} \sqrt{\frac{2}{\pi}} \sigma_f^{-1} \int_0^\infty d \left(\frac{V}{\sigma_f} \right) \left(\frac{V}{\sigma_f} \right)^3 e^{-V^2/2\sigma_f^2} \langle \delta v_x \rangle. \quad (70)$$

This quantity was computed after scaling the velocity changes obtained from the scattering experiments, given assumed values for the two dimensionless parameters

$$R \equiv \frac{p_{max}}{p_f}, \quad S \equiv \frac{V_{bin}}{\sigma_f}, \quad (71)$$

with $p_f = GM_{12}/\sigma_f^2$; the parameter S measures the hardness of the binary. Figure 6 shows $R_1 \equiv A(R, S)/A_C$, the dynamical friction coefficient for the binary normalized by the point-mass coefficient (equation 47a). Values of $p_{max} \lesssim a$ are not physically interesting, hence R and S are restricted to $R > 1/S^2$. The greatest reduction in the frictional force occurs at small R and S . Small R corresponds to low p_{max} , hence to a small contribution of distant encounters to $\langle \Delta v_{\parallel} \rangle$. Small S implies a wide binary (in comparison with p_{max} , say) and hence a larger fraction of stars that interact strongly with the binary. In the case $R \approx 1$, i.e. $p_{max} \approx p_f$, we see that the reduction in the frictional force is $\sim 50\%$ for the widest binaries, $V_{bin} \approx \sigma_f$, falling to $\sim 20\%$ for $V_{bin} = 2\sigma_f$ and $\sim 5\%$ for $V_{bin} = 5\sigma_f$.

Results presented so far were averages over all orientations of the binary's orbital plane with respect to the initial velocity of the field star, and the direction of the binary's center-of-mass motion. In reality, the binary will have a particular orientation with respect to its center-of-mass motion, at least on time scales short compared to the time required for the orientation of the binary or its direction of motion to change. The typical velocity change of an interacting field star would be expected to depend systematically on the angle Ψ between the normal to the binary orbital plane and \mathbf{V} . Figure 7 illustrates the dependence $D_1(\Psi, p_{max})$ for the case $V = 1.0 \times \sqrt{GM_{12}/a}$. The dynamical friction force is greatest when the binary orbital plane is perpendicular to the relative velocity vector, although the dependence on Ψ is mild. In the case of low impact parameters, $p_{max} \lesssim a$, and $\Psi \approx 0$, the frictional force is close to zero since the field stars pass through the middle of the binary at high enough velocity that almost no deflection takes place.

4.2. Diffusion

We may similarly define dimensionless ratios D_2 and D_3 between the diffusion coefficients $\langle \delta v_x^2 \rangle$ and $\langle \delta v_y^2 + \delta v_z^2 \rangle$ computed from the binary scattering experiments, and their equivalents for a point-mass scatterer, equations (53a) and (53b):

$$D_2(V, p_{max}) = \frac{1 + p_{max}^2/p_0^2}{4p_{max}^2/p_0^2} \left(\frac{V}{V_{bin}} \right)^2 \int_0^{p_{max}/a} d \left(\frac{p}{a} \right)^2 \left(\frac{\overline{\delta v_x^2}}{V_{bin}} \right), \quad (72a)$$

$$D_3(V, p_{max}) = \frac{1 + p_{max}^2/p_0^2}{4[(1 + p_{max}^2/p_0^2) \ln(1 + p_{max}^2/p_0^2) - p_{max}^2/p_0^2]} \left(\frac{V}{V_{bin}} \right)^2 \times \int_0^{p_{max}/a} d \left(\frac{p}{a} \right)^2 \left(\frac{\overline{\delta v_y^2 + \delta v_z^2}}{V_{bin}} \right). \quad (72b)$$

Figures 8 and 9 plot D_2 and D_3 as functions of p_{max} and V . The coefficient D_2 describes mean square changes in the binary's velocity parallel to \mathbf{V} ; these are non-dominant, i.e. bounded in their integration over impact parameter at large p_{max} . Hence D_2 does not tend toward unity at large p_{max} . At small p_{max} , the expected change in v_{fx} for scattering off a point mass is $\sim -2V$ (equation 52), whereas a typical change after interaction with the binary is $\sim -0.5\sqrt{GM_{12}/a}$ (cf. Fig. 5). These are comparable when $V \approx 0.25V_{bin}$; thus for $V \lesssim 0.25V_{bin}$ one expects $D_2 \gtrsim 1$ for all p_{max} , while for $V \gtrsim 0.25V_{bin}$ one expects $D_2 \lesssim 1$ for all p_{max} , in good agreement with Figure 8. For sufficiently large V , D_2 drops to zero at small p_{max} since most field stars pass through the binary without significant change in velocity.

D_3 describes the mean square change in the binary's velocity perpendicular to \mathbf{V} , which diverges as $\ln p_{max}$ in the case of a point-mass perturber (equation 53b); thus $D_3 \rightarrow 1$ in the limit of large p_{max} . For small p , the change in v_{fy} for a

point-mass scatterer goes to zero (cf. equation 52), while δv_f^2 remains finite in the case of interactions with the binary; hence D_3 diverges at small p_{max} .

The diffusion coefficients for the binary are

$$C = \sqrt{\frac{2}{\pi}} \int_0^\infty d\left(\frac{V}{\sigma_f}\right) \left(\frac{V}{\sigma_f}\right)^2 e^{-V^2/2\sigma_f^2} \langle \delta v_x^2 \rangle, \quad (73a)$$

$$2E = \sqrt{\frac{2}{\pi}} \int_0^\infty d\left(\frac{V}{\sigma_f}\right) \left(\frac{V}{\sigma_f}\right)^2 e^{-V^2/2\sigma_f^2} \langle \delta v_y^2 + \delta v_z^2 \rangle. \quad (73b)$$

Figure 10 plots the ratio $R_2 = (C + 2E)/(C_C + 2E_C)$ between $\langle \Delta v^2 \rangle$ for the binary and for a point-mass perturber in the low- v limit (cf. §2). The dashed line in that figure is

$$1 + \frac{H}{32\sqrt{2\pi} \ln \sqrt{1 + 2R^2}}, \quad (74)$$

the expected ratio in the limit of an infinitely hard binary according to the approximate treatment of §1, equation (12); $\ln \Lambda$ in that expression was replaced by $\ln \sqrt{1 + 2R^2}$ (eq. 49) and the hardening rate H was set to 15, appropriate for a hard binary (Hills 1983; Quinlan 1996). The computed curves may be seen to tend toward the analytic expression as $S = V_{bin}/\sigma_f$ increases, i.e. as the binary becomes harder.

Finally, Figure 11 gives the ratio $\sigma/\sigma_C = (R_2/R_1)^{1/2}$, the factor by which the equilibrium velocity dispersion of the binary is increased relative to that of a point mass with $M = M_{12}$. Based on equation (74), this ratio is expected to be

$$\frac{\sigma}{\sigma_C} \approx \sqrt{1 + \frac{0.18}{\ln \sqrt{1 + 2R^2}}}, \quad (75)$$

in the limit of a hard binary; this estimate ignores the additional contribution to the random motion from the reduction in dynamical friction discussed above. Equation (75) is plotted in Figure 11. At fixed p_{max} , Figure 11 implies that σ/σ_C will increase with increasing hardness of the binary, until reaching a limiting value similar to equation (75). Thus the wandering of the binary should increase slightly in amplitude as its semi-major axis shrinks.

The results of this section may be summarized as follows. The velocity-dependent dynamical friction coefficient $D_1(V)$ for a binary (Figure 4), with V the velocity of the field star at infinity, is typically less than that for a point particle due to randomization of the direction in which field stars are ejected during close encounters (Figure 5). The velocity-dependent diffusion coefficient $D_3(V)$ (Figure 9) is typically greater than that for a point particle due to the gain of energy which a field star experiences during a close encounter. After averaging over field-star velocities, the dynamical friction and diffusion coefficients for the binary, $\langle \Delta v_{\parallel} \rangle$ and $\langle \Delta v^2 \rangle$, are respectively less (in absolute value) and greater than their values for a point particle (Figure 6 and 10). Both effects act to increase the random velocity of a binary in equilibrium with field stars compared to the equilibrium random velocity of a point particle of the same mass (Figure 11). However the increase is modest unless $R \equiv p_{max}/p_f = p_{max}\sigma_f^2/GM_{12}$ is less than about one, in other words, unless the maximum effective impact parameter for gravitational encounters p_{max} in Chandrasekhar's theory is of order the radius of gravitational influence of the binary GM_{12}/σ_f^2 .

5. DISCUSSION

5.1. Estimating p_{max}/p_f

The results presented above, in particular equation (75) and Figure 11, demonstrate that the random motion of a massive binary will be dominated by distant (elastic) encounters and therefore essentially the same as the Brownian motion of a point particle, unless the ratio

$$R \equiv \frac{p_{max}}{p_f} = \frac{p_{max}\sigma_f^2}{GM_{12}} \quad (76)$$

is smaller than about one. The motivation for this result was presented already in the Introduction: the net effect of distant (elastic) encounters is proportional to $\ln \Lambda \approx \ln \sqrt{1 + 2R^2}$ (cf. equation 48), hence R must be small for close (inelastic) encounters to dominate.

If the massive binary is located in a constant density region of radius $\sim r_c$ at the center of a stellar system with a steeply falling density profile, then $p_{max} \approx r_c$ (Appendix A).

To estimate p_f , we note that $p_f \approx r_G$, the radius of gravitational influence of a body of mass M_{12} embedded in a stellar system with velocity dispersion σ_f . In most applications of Chandrasekhar's theory, p_f is smaller than p_{max} by orders of magnitude and $R \gg 1$. For instance, scaling to parameters appropriate to stars in a globular cluster,

$$p_f \equiv \frac{GM}{\sigma_f^2} \approx \frac{Gm_f}{\sigma_f^2} \approx 4.3 \times 10^{-5} \text{pc} \left(\frac{\sigma_f}{10 \text{ km s}^{-1}} \right)^{-2} \left(\frac{m_f}{M_{\odot}} \right), \quad (77)$$

much smaller than a core radius of ~ 1 pc. However in the situations of interest here, p_f is larger, and R smaller, by roughly a factor $M_{12}/m_f \gg 1$ (ignoring changes in σ_f). In the case of a binary consisting of two $10M_\odot$ black holes in a globular cluster, we have

$$p_f \approx 10^{-3} \text{pc} \left(\frac{\sigma_f}{10 \text{ km s}^{-1}} \right)^{-2} \left(\frac{M_{12}}{20M_\odot} \right). \quad (78)$$

In the case of a supermassive black hole binary at the center of a galaxy, we can use the $M_\bullet - \sigma$ relation

$$M_{12} = M_\bullet \approx 1.30 \times 10^8 M_\odot \left(\frac{\sigma_f}{200 \text{ km s}^{-1}} \right)^{4.7} \quad (79)$$

(Merritt & Ferrarese 2001) to write

$$p_f \approx 10 \text{ pc} \left(\frac{\sigma_f}{200 \text{ km s}^{-1}} \right)^{2.7}. \quad (80)$$

Consider first a binary black hole at the center of a globular cluster. A core radius of $r_c \approx 1$ pc is still much greater than $p_f \approx 10^{-3}$ pc, implying $R \gg 1$ and no appreciable enhancement of the Brownian motion. However in the “post-core-collapse” globular clusters (Djorgovski & King 1986) the stellar density follows a steep power law all the way into the observable center and r_c is much smaller than 1 pc. While p_{max} is not well defined in this case, arguments like those in the Appendix suggest that the effective p_{max} would be small, hence $R \lesssim 1$ and a substantial enhancement in the Brownian motion is predicted (Figure 11).

Next consider the case of a $\sim 10^8 M_\odot$ black-hole binary in a galactic nucleus. Like globular clusters, some galaxy nuclei have “cores” (Lauer et al. 1995), actually weak power laws in the space density (Merritt & Fridman 1996). (The cores of globular clusters could also be weak power laws.) The “break radius” r_b in these galaxies (Faber et al. 1997) plays roughly the role of a core radius; Poon & Merritt (2000) note that $r_b \approx$ a few $\times r_G$ in two galaxies where both r_b and M_\bullet can be accurately measured, hence $p_{max} \gtrsim p_f$ and $R \gtrsim 1$. In the “power-law” galaxies (Ferrarese et al. 1994; Lauer et al. 1995), which have no detectable core, R would be smaller, $R \lesssim 1$. The enhancement of the Brownian motion could be substantial for a massive binary at the center of a power-law galaxies, perhaps as much as a factor of two in σ (Figure 11).

The concept of a maximum effective impact parameter p_{max} on which these estimates depend is a loose one, both as used here and in Chandrasekhar’s original theory. Refining these estimates of p_{max} will require N -body simulations.

5.2. Equilibration time scales

Here we test the assumption made above (§2) that the center-of-mass motion of the binary reaches a statistical steady state in a time short compared to the time over which the orbital elements of the binary change. In fact this is not always the case. The time scale for change of the binary’s semi-major axis (cf. equation 7) is

$$t_{\text{harden}} \equiv \left[a \frac{d}{dt} \left(\frac{1}{a} \right) \right]^{-1} = \frac{\sigma_f}{G \rho_f a H}. \quad (81)$$

Approach to statistical equilibrium of the Brownian motion occurs in a time (cf. equation 18c)

$$t_{\text{harden}} \equiv \left| \frac{v}{\langle \Delta v_{\parallel} \rangle} \right| \approx \left| \frac{v^2}{\langle \Delta v^2 \rangle} \right| \approx \frac{1}{A} \approx \frac{1}{A_c} = \frac{3}{4\sqrt{2\pi}} \frac{\sigma_f^3}{G^2 M_{12} \rho_f \ln \Lambda}. \quad (82)$$

The ratio is

$$\frac{t_{\text{harden}}}{t_{\text{relax}}} = \frac{4\sqrt{2\pi}}{3H} \frac{GM_{12}}{a\sigma_f^2} \ln \Lambda = \frac{4\sqrt{2\pi} S^2 \ln \Lambda}{3H} \approx \frac{3.3 S^2 \ln \sqrt{1+R^2}}{H} \quad (83)$$

with $S^2 \equiv V_{\text{bin}}^2/\sigma_f^2 = GM_{12}/\sigma_f^2 a$. This ratio must be large if the binary’s semi-major axis is to remain nearly fixed during the time required for the Brownian motion to be established. For large enough R , i.e. large enough p_{max} , this is guaranteed. However the case of most interest here is $R \approx 1$ (§5.1), for which

$$\frac{t_{\text{harden}}}{t_{\text{relax}}} \approx \frac{S^2}{H}. \quad (84)$$

For a very hard binary, $H \approx 15$ (Quinlan 1996) and $t_{\text{decay}}/t_{\text{relax}} \approx 0.07 V_{\text{bin}}^2/\sigma_f^2$, which exceeds unity for $S = V_{\text{bin}}/\sigma_f \gtrsim 4$. Thus the condition is satisfied for sufficiently hard binaries. For a soft binary, $S \lesssim 1$, we can use the expressions in Quinlan (1966, eqs. 16-18), to write $H \approx 4.4 S^2$, giving $t_{\text{decay}}/t_{\text{relax}} \approx 0.23$. Thus in the case of a soft binary, the binary separation *will* change appreciably during the time that the Brownian motion is being established. However in the soft regime, the Brownian velocity dispersion depends only very weakly on S (cf. Figure 11), so the conclusions presented above are not significantly affected.

5.3. *Consequences of Brownian motion*

The Brownian velocity dispersion of the binary is predicted to be (equation 27)

$$\langle v^2 \rangle = 3\sigma^2 = 3 \frac{R_2}{R_1} \frac{m_f}{M_{12}} \sigma_f^2. \quad (85)$$

We can convert this into a mean square displacement by assuming that the binary moves in a harmonic potential well produced by a uniform density core of field stars. The virial theorem

$$\langle v^2 \rangle = -\langle \mathbf{F} \cdot \mathbf{r} \rangle \quad (86)$$

as applied to the binary's center-of-mass motion relates the mean square velocity of the binary to an average of the force acting on it. In a spherical constant-density core, the force (neglecting encounters) is $-(4\pi G\rho_f/3)\mathbf{r}$ and

$$\langle v^2 \rangle = \frac{4}{3} \pi G \rho_f \langle r^2 \rangle. \quad (87)$$

Writing $r_c^2 = 9\sigma_f^2/4\pi G\rho_f$ (King 1966) yields

$$\frac{\langle r^2 \rangle}{r_c^2} = \frac{R_2}{R_1} \frac{m_f}{M_{12}}. \quad (88)$$

This treatment (cf. Bahcall & Wolf 1976) is approximate in that it ignores the effect of the motion of the binary on the background stars and assumes that gravitational encounters are uncoupled from the quasi-periodic motion in the core.

For a binary black hole at the center of a globular cluster, the rms Brownian velocity is

$$v_{rms} \approx 3.87 \text{ km s}^{-1} \left(\frac{R_2}{R_1} \right)^{1/2} \left(\frac{20m_f}{M_{12}} \right)^{1/2} \left(\frac{\sigma_f}{10 \text{ km s}^{-1}} \right) \quad (89)$$

and the wandering radius is

$$r_{rms} \approx 0.22 \text{ pc} \left(\frac{R_2}{R_1} \right)^{1/2} \left(\frac{20m_f}{M_{12}} \right)^{1/2} \left(\frac{r_c}{1 \text{ pc}} \right). \quad (90)$$

In the case of a binary supermassive black hole in a galactic nucleus, the Brownian velocity is only

$$v_{rms} \approx 0.030 \text{ km s}^{-1} \left(\frac{R_2}{R_1} \right)^{1/2} \left(\frac{m_f}{M_\odot} \right)^{1/2} \left(\frac{\sigma_f}{200 \text{ km s}^{-1}} \right)^{-1.35} \quad (91)$$

and the wandering radius is

$$r_{rms} \approx 0.0087 \text{ pc} \left(\frac{R_2}{R_1} \right)^{1/2} \left(\frac{\sigma_f}{200 \text{ km s}^{-1}} \right)^{-2.35} \left(\frac{r_c}{100 \text{ pc}} \right); \quad (92)$$

the $M_\bullet - \sigma$ relation (79) has again been used to relate M_{12} to σ_f . The Brownian motion of a supermassive black hole is of course very small, even with the enhancement due to inelastic scattering derived here. The predicted wandering radius is smaller than the likely separation of the black holes in a binary system; in fact it is of order the separation at which gravitational radiation would lead to a rapid coalescence (Merritt 2000).

Measurement of the velocity of the Milky Way black hole has recently become feasible (Reid et al. 1999; Backer & Sramek 1999). The upper limit of $\sim 20 \text{ km s}^{-1}$ is a factor ~ 200 greater than the expected Brownian velocity given its mass of $\sim 3 \times 10^6 M_\odot$.

The wandering amplitude of a binary supermassive black hole in a galactic nucleus has recently been discussed by a number of authors (Makino 1997; Quinlan & Hernquist 1997; Merritt 2000; Gould & Rix 2000). The problem is interesting because a stationary black-hole binary will quickly eject all of the stars with pericenters less than $\sim 2a$ (e.g. Zier 2000); once this occurs, the density of stars around the binary drops and the decay stalls. Wandering is a possible way to increase the number of stars that a binary can interact with, thus allowing the binary to decay to the point that gravitational radiation coalescence can occur (Peters 1964).

Quinlan & Hernquist (1997), in a series of computer simulations using a hybrid N -body code, noticed a wandering of a massive binary with an amplitude more than five times greater than expected on the basis of an equation like (92). The core radius that they cite, ~ 0.04 , is comparable to r_G in their simulations, so $R \approx r_c/r_G \approx 1$. Figure 11 suggests that the increase in the amplitude of the wandering would probably be much less than the claimed factor of 5–10.

Makino (1997) carried out N -body merger simulations similar to those of Quinlan & Hernquist (1997) but using a more conservative, direct-summation code. Makino's Figure 7 shows a wandering amplitude that scales as $\sim N^{-1/2}$; the rms velocity of the binary in that plot is comparable, or perhaps $\sim 50\%$ larger, than expected for a point mass, consistent with the results obtained here.

Quinlan & Hernquist (1997) used a spectrum of masses for the field particles, spanning a range of $\sim 10^3$ in m_f , and adopted the lowest mass when computing the expected amplitude of the binary's Brownian motion. Mass segregation might have brought some of the more massive particles into the nucleus over the course of their simulations. Quinlan & Hernquist also used a basis-function-expansion code for computing the forces between field stars. Such codes do not conserve momentum and this too may have contributed to the random motion of the binary. A repeat of the Quinlan & Hernquist simulations using a different N -body code could help to clarify the discrepancy between their results and those of Makino.

If supermassive black hole binaries wander as little as implied by equations (75) or (92), it is difficult to see how they could interact with enough stars to allow them to achieve gravitational-radiation coalescence in a reasonable time (Merritt 2000). Unless some other mechanism is effective at removing energy from these binaries, one might expect them to persist for the lifetime of a galaxy at separations $a \lesssim 0.1$ pc, or at least until a subsequent merger event brings another supermassive black hole into the nucleus (Valtonen 1996).

I thank Miloš Milosavljević for advice about evaluating some of the integrals and for numerous discussions about the ideas presented here. A conversation with Douglas Heggie helped to motivate this paper. This work was supported by NSF grants AST 96-17088 and 00-71099 and by NASA grants NAG5-6037 and NAG5-9046.

APPENDIX

Maoz (1993, eq. 4.4) gives an implicit expression for p_{max} appropriate for an object at the center of a spherically-symmetric matter distribution $\rho(r)$. Maoz's formula,

$$\frac{1}{\rho(0)} \int_{p_{min}}^{\infty} \frac{\rho(r)}{r} dr, \quad (\text{A1})$$

replaces the Coulomb logarithm in expressions like equation (21a). If we set

$$\rho(r) = \rho(0) \left(1 + \frac{r^2}{r_c^2}\right)^{-\gamma/2}, \quad (\text{A2})$$

with r_c the core radius of the field stars, Maoz's formula gives

$$\ln \Lambda \approx \begin{cases} \sinh^{-1} \left(\frac{r_c}{p_{min}} \right) & \text{if } \gamma = 1, \\ \frac{1}{2} \ln \left(\frac{p_{min}^2 + r_c^2}{p_{min}^2} \right) & \text{if } \gamma = 2. \end{cases} \quad (\text{A3})$$

Setting $p_{min} \approx p_f \approx GM_{12}/\sigma_f^2$ (eq. 50) and equating $\ln \Lambda$ with $\ln \sqrt{1 + 2R^2}$ (eq. 49), we find

$$R \approx \frac{r_c}{p_f} \approx \frac{r_c}{r_G} \quad (\text{A4})$$

for both values of γ .

REFERENCES

- Alcock, C. et al. 1997, *ApJ*, 486, 697
 Backer, D. C. & Sramek, R. A. 1999, *ApJ*, 520, 137
 Bahcall, J. N. & Wolf, R. A. 1976, *ApJ*, 209, 214
 Begelman, M. C., Blandford, R. D. & Rees, M. J. 1980, *Nature*, 287, 307
 Carr, B. J., Bond, J. R. & Arnett, W. D. 1984, *ApJ*, 277, 445
 Chandrasekhar, S. 1942, *Principles of Stellar Dynamics* (Chicago: Univ. of Chicago Press)
 Chandrasekhar, S. 1943a, *ApJ*, 97, 255
 Chandrasekhar, S. 1943b, *Rev. Mod. Phys.*, 15, 1
 Djorgovski, S. & King, I. 1986, *ApJ*, 305, L61
 Ebisuzaki, T., Makino, J. & Okumura, S. K. 1991, *Nature*, 354, 212
 Einstein, A. 1955, *Investigations on the Theory of Brownian Motion* (New York: Dover)
 Faber, S. M. et al. 1997, *AJ*, 114, 1771
 Ferrarese, L., & Merritt, D. 2000, *ApJ*, 539, L9
 Ferrarese, L., van den Bosch, F. C., Ford, H. C., Jaffe, W. & O'Connell, R. W. 1994, *AJ*, 108, 1598
 Gebhardt, K. et al. 1996, *AJ*, 112, 105
 Gould, A. & Rix, H.-W. 2000, *ApJ*, 532, 29
 Hairer, E., Nørsett, S. P. & Wanner, G. 1991, *Solving Ordinary Differential Equations I. Nonstiff Problems* (Berlin: Springer)
 Heggie, D. C. 1975, *MNRAS*, 173, 729
 Hénon, M. 1973, in *Dynamical Structure and Evolution of Stellar Systems*, ed. L. Martinet & M. Mayor (Geneva: Geneva Observatory), 183
 Hills, J. G. 1983, *AJ*, 88, 1269
 Hills, J. G. 1992, *AJ*, 103, 1955
 Hills, J. G. & Fullerton, L. W. 1980, *AJ*, 85, 1281
 Hut, P. & Rees, M. J. 1992, *MNRAS*, 259, 27
 King, I. R. 1966, *AJ*, 71, 64
 Lacey, C. G. & Ostriker, J. P. 1985, *ApJ*, 299, 33
 Lauer, T. R. et al. 1995, *AJ*, 110, 2622
 Makino, J. 1997, *ApJ*, 478, 58
 Maoz, E. 1993, *MNRAS*, 263, 75
 Merritt, D. 2000, in *Dynamics of Galaxies: from the Early Universe to the Present*, eds. F. Combes, G. A. Mamon, & V. Charmandaris (ASP Conference Series, Vol. 197), p. 221.
 Merritt, D., & Ferrarese, L. 2001, *ApJ*, 547, 140
 Merritt, D. & Fridman, T. 1996, in *Fresh Views of Elliptical Galaxies*, eds. A. Buzzoni, A. Renzini & A. Serrano (ASP Conference Series, Vol. 86), p. 13.
 Mikkola, S. & Valtonen, M. J. 1992, *MNRAS*, 259, 115
 Nakamura, T., Sasaki, M., Tanaka, T. & Thorne, K. S. 1997, *ApJ*, 487, L139
 Peters, P. C. 1964, *Phys. Rev. B.*, 136, 1224
 Poon, M. & Merritt, D. 2001, *ApJ*, in press (astro-ph/0006407)
 Portegies Zwart, S. & McMillan, S. L. W. 1999, astro-ph/9912022
 Portegies Zwart, S. & McMillan, S. L. W. 2000, *ApJ*, 528, L17
 Quinlan, G. D., 1996, *NewA*, 1, 35
 Quinlan, G. D. & Hernquist, L. 1997, *New A*, 2, 533
 Reid, M. J., Readhead, A. C. S., Vermeulen, R. C. & Treuhaft, R. N. 1999, *ApJ*, 524, 81
 Rosenbluth, M. N., MacDonald, W. M. & Judd, D. L. 1957, *Phys. Rev.*, 107, 1
 Spitzer, L. 1987, *Dynamical Evolution of Globular Clusters* (Princeton: Princeton Univ. Press)
 Valtonen, M. J. 1996, *Comm. Ap.*, 18, 191
 van Kampen, N. G. 1992, *Stochastic Processes in Physics and Chemistry* (Amsterdam: North-Holland)
 White, M. L. 1949, *ApJ*, 109, 159
 Young, P. J. 1977, *ApJ*, 215, 36
 Zier, C. 2000, PhD thesis, Univ. Bonn

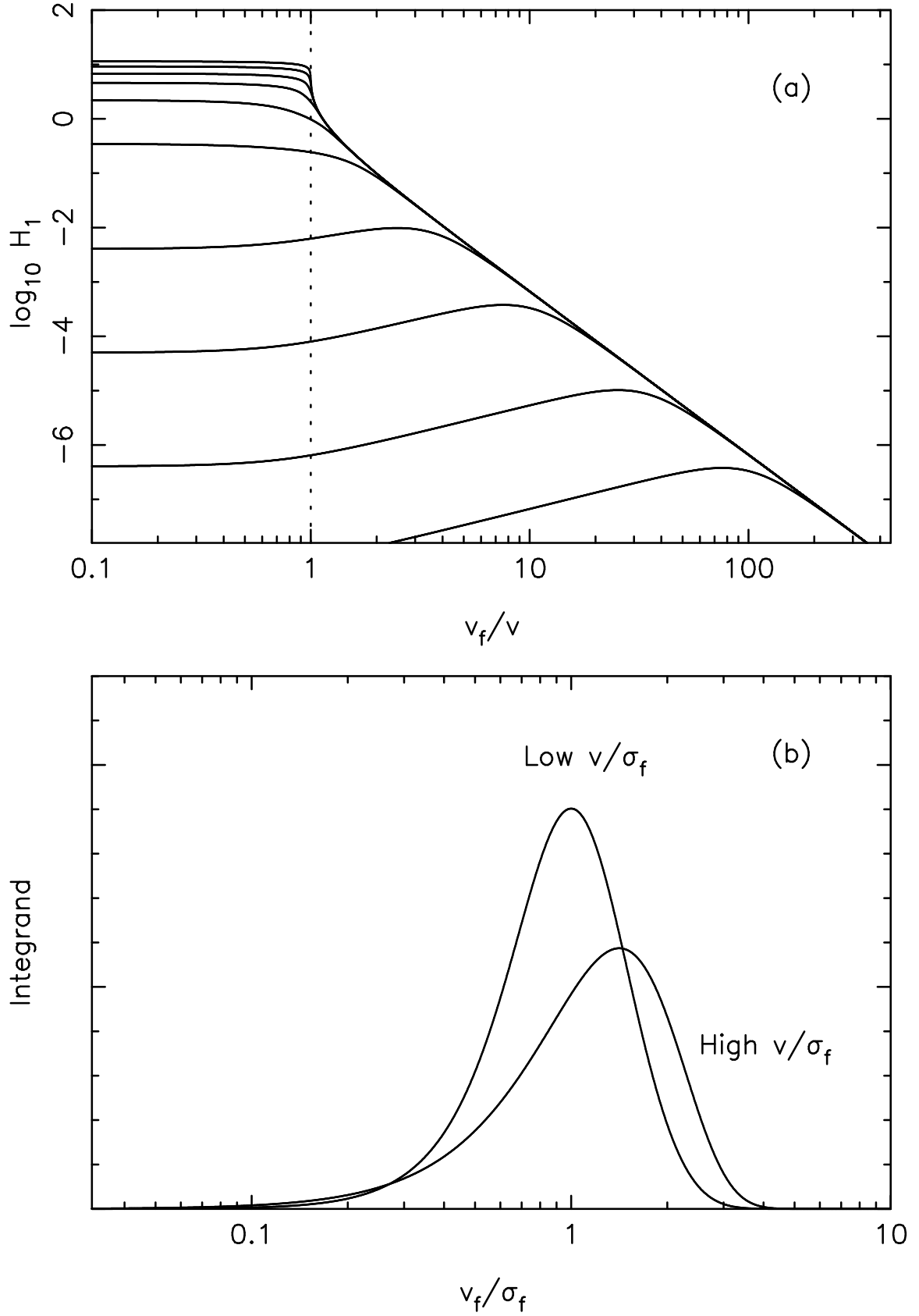


FIG. A1.— (a) $H_1(v, v_f, p_{max})$, equation (36), for $p_{max}/p_f = 1$ and $v/\sigma_f = \{0.01, 0.03, 0.1, 0.3, 1, 3, 10, 30, 100, 300\}$; v/σ_f increases upwards. (b) The relative contribution of different field-star velocities to the dynamical friction integral (34), in the limit of low and high test-star velocities.

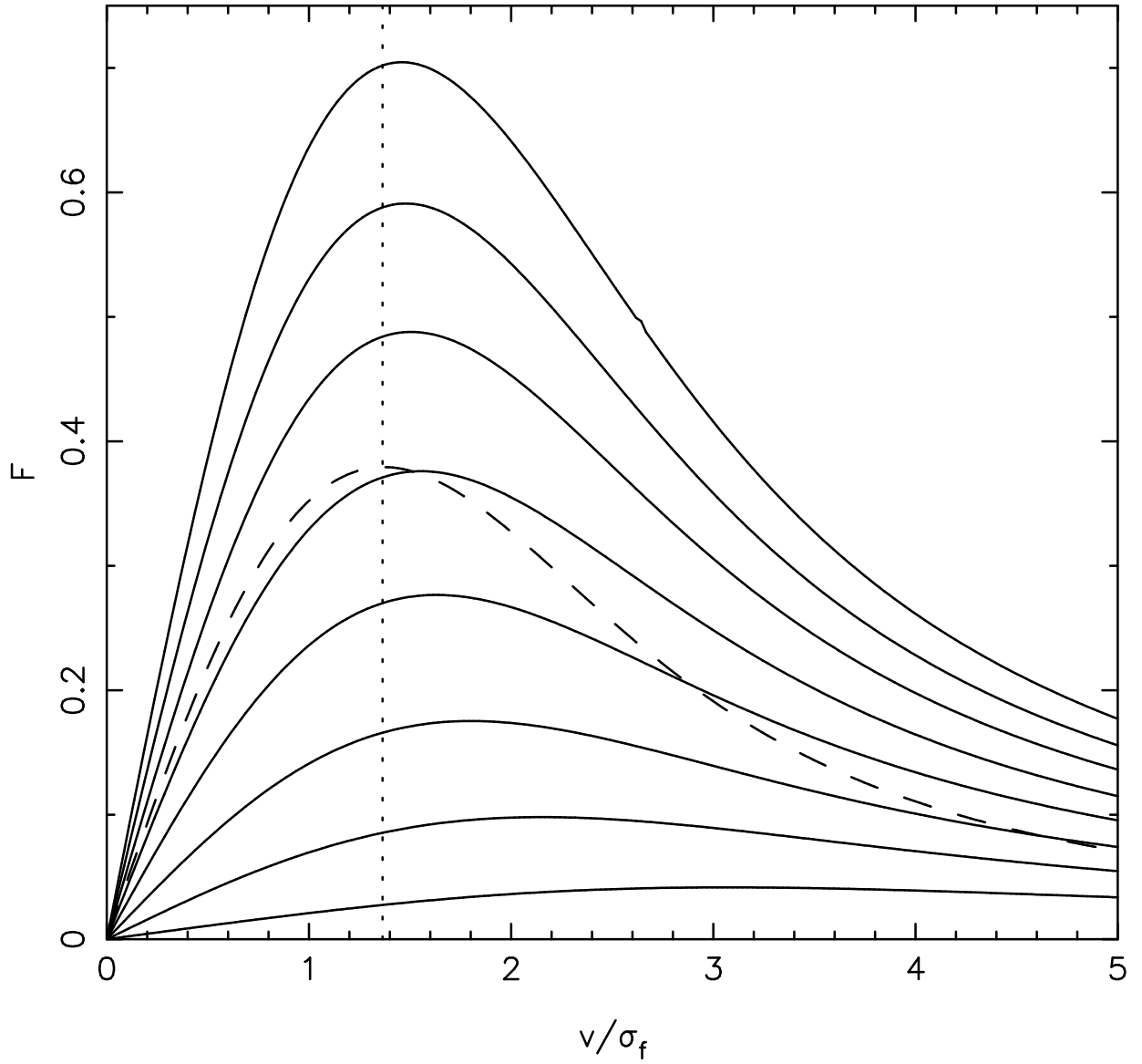


FIG. A2.— The dimensionless dynamical friction coefficient $F(v, p_{max})$ (equation 41b) for $p_{max}/p_f = \{0.3, 1, 3, 10, 30, 100, 300, 1000\}$. Dashed curve is the classical expression with $\ln \Lambda = 4$; vertical dotted line indicates the position of the maximum of this function.

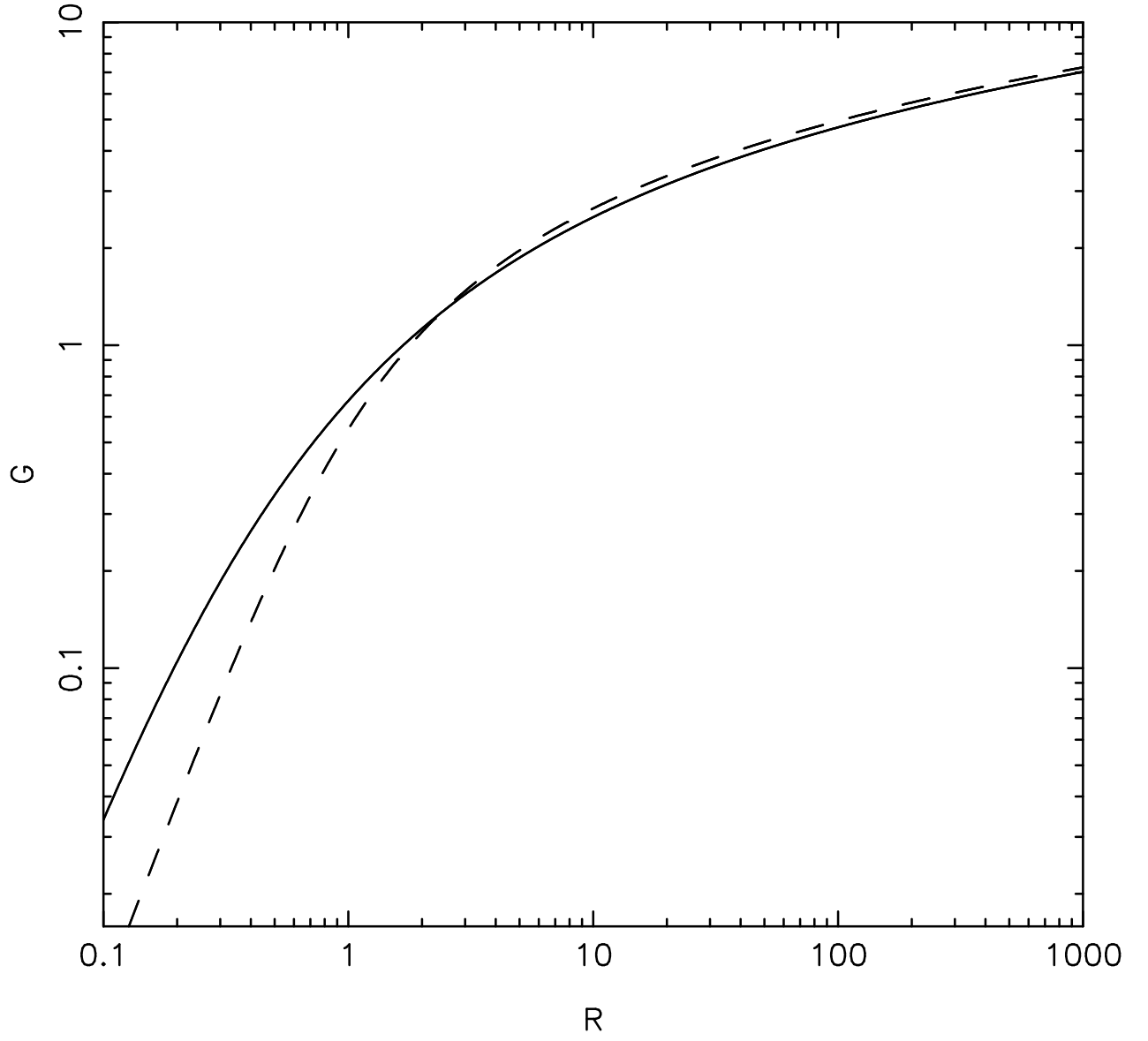


FIG. A3.— The function $G(R)$ (equation 47b). The dashed line is the approximation of equation (48), $G(R) \approx \ln \sqrt{1 + 2R^2}$.

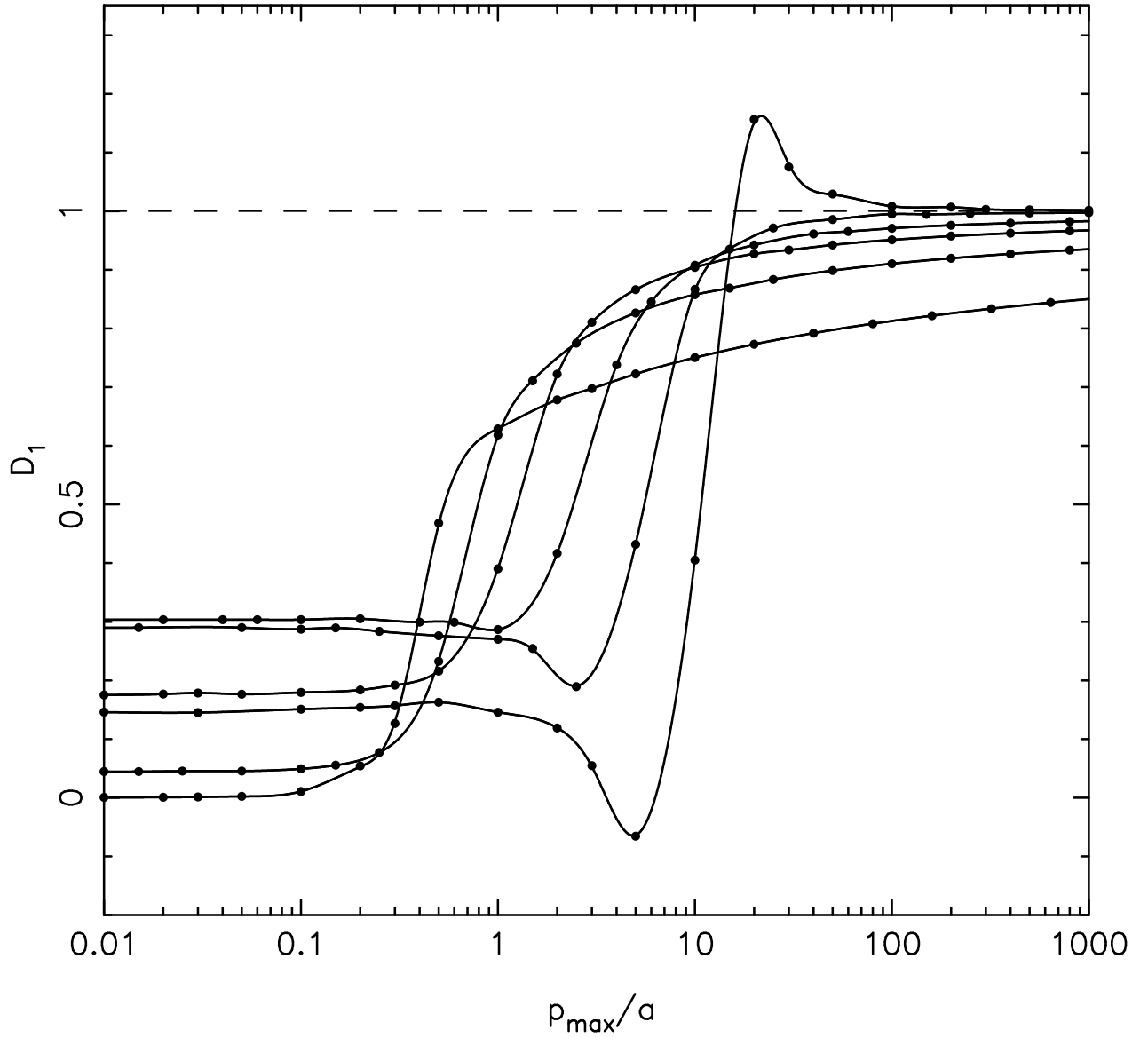


FIG. A4.— Dynamical friction reduction factor $D_1(V, p_{max})$ (eq. 67b). D_1 is defined as the mean change in field-star velocities after interaction with the binary, expressed as a fraction of the value expected for interactions with a point-mass scatterer of the same total mass as the binary; p_{max} is the maximum impact parameter and a is the binary semi-major axis. Different curves correspond to relative velocities at infinity of $V/V_{bin} = 0.1, 0.2, 0.5, 1, 2, 10$; the lowest (highest) V produces the highest (lowest) D_1 at large p_{max} . Points are averages computed from the numerical integrations; curves are spline fits. Some of the curves have been extended to large p_{max}/a using the analytic expression for a point-mass scatterer.

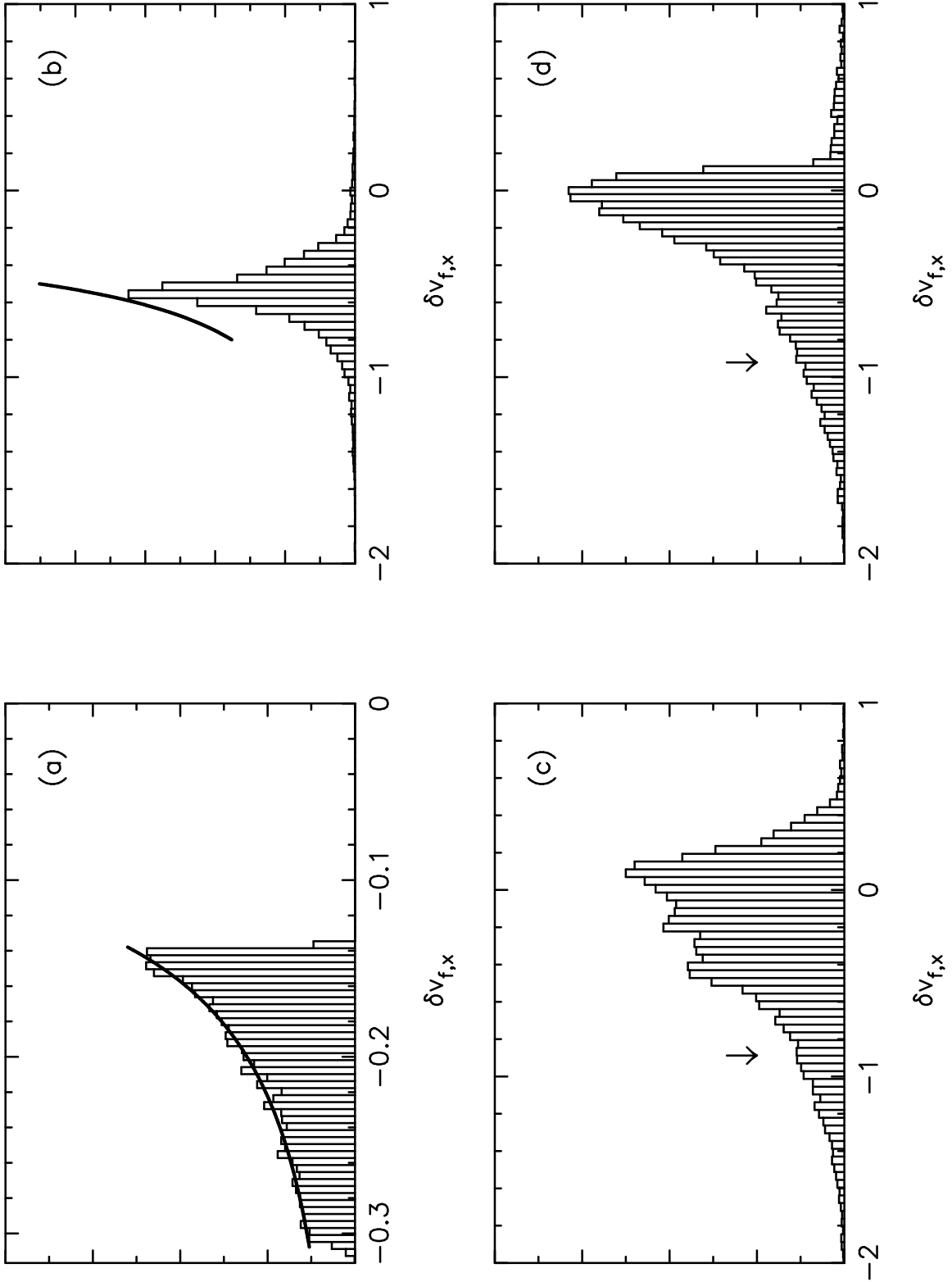


FIG. A5.— Distribution of field star velocity changes for scattering experiments with $V/V_{bin} = 0.5$. Each plot corresponds to 5×10^4 scattering experiments within some range of impact parameters $[p_1, p_2]$ in units of a . (a) $[6, 10]$ (b) $[2, 4]$ (c) $[0.6, 1]$ (d) $[0.4, 0.6]$. Solid lines in (a) and (b) are the distributions corresponding to scattering off a point-mass perturber. In (c) and (d), the mean of this distribution (which is very narrow) is indicated by the arrows. The magnitude of the frictional force is proportional to the mean value of $-\delta v_{f,x}$; at low impact parameters, the distribution of $\delta v_{f,x}$'s is shifted toward zero and the frictional force is reduced.

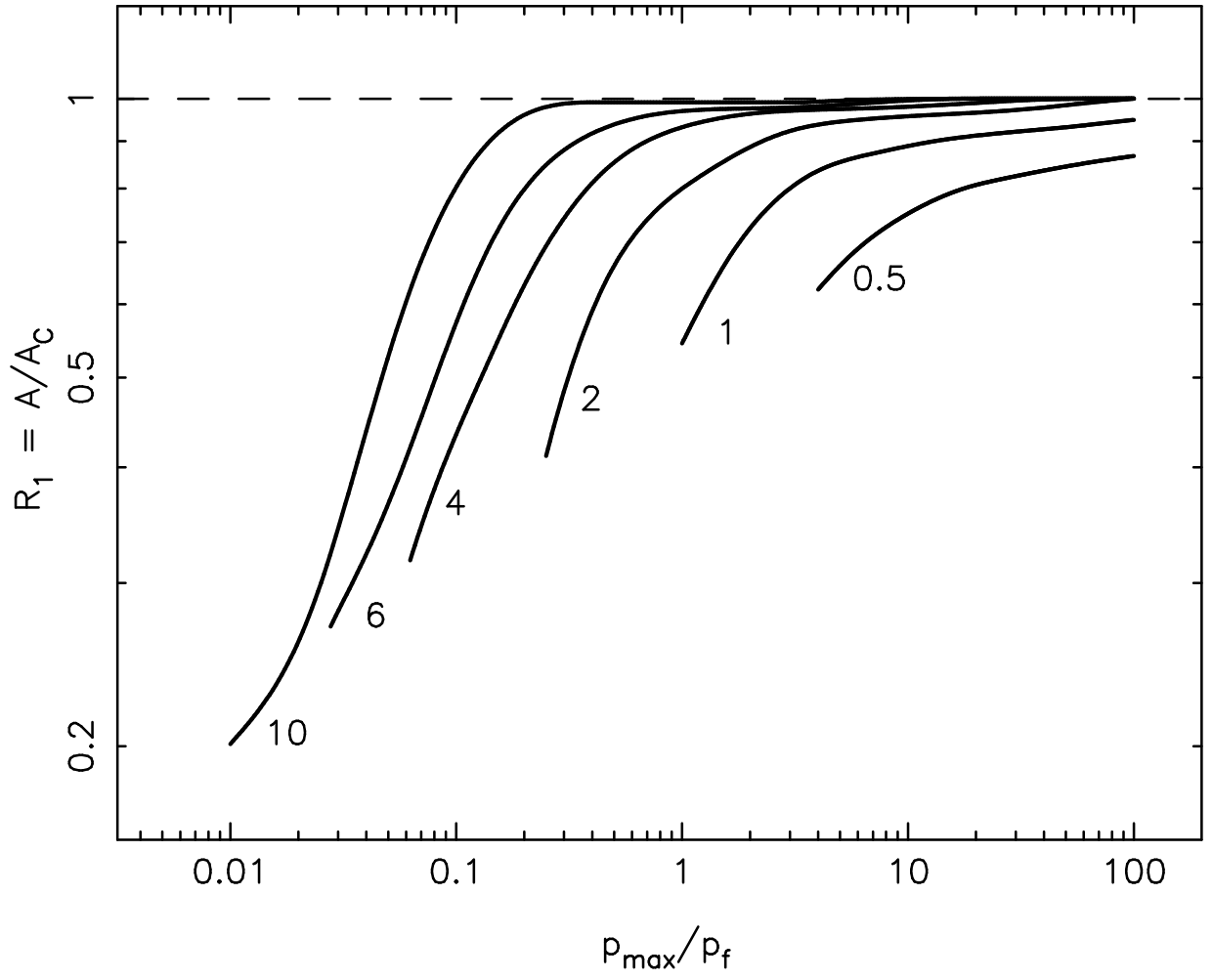


FIG. A6.— Reduction in the dynamical friction force for a massive binary moving at low velocity, $v \ll \sigma_f$. Different curves correspond to $V_{bin}/\sigma_f = 0.5, 1, 2, 5, 10$; the lowest (highest) V_{bin} produces the the highest (lowest) reduction factor at large p_{\max}/p_f .

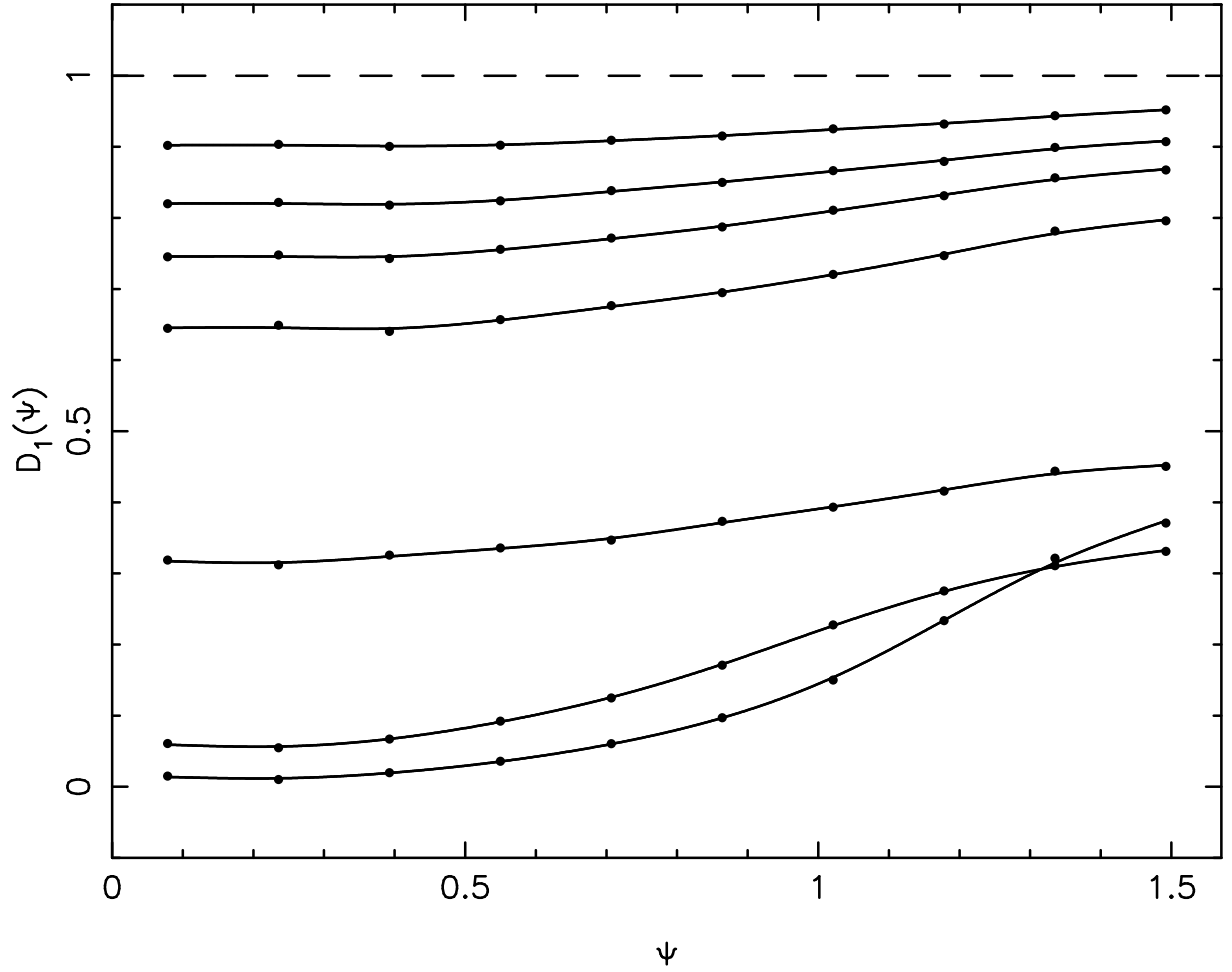


FIG. A7.— Dynamical friction reduction factor as a function of angle Ψ between the normal to the binary's orbital plane and the relative velocity vector of the field stars, for $V/V_{bin} = 1$. Different curves correspond to different values of the maximum impact parameter; proceeding upward, $p_{max}/a = (0.2, 0.5, 1, 2, 3, 5, 20)$. Points are averages computed from the numerical integrations; curves are spline fits.

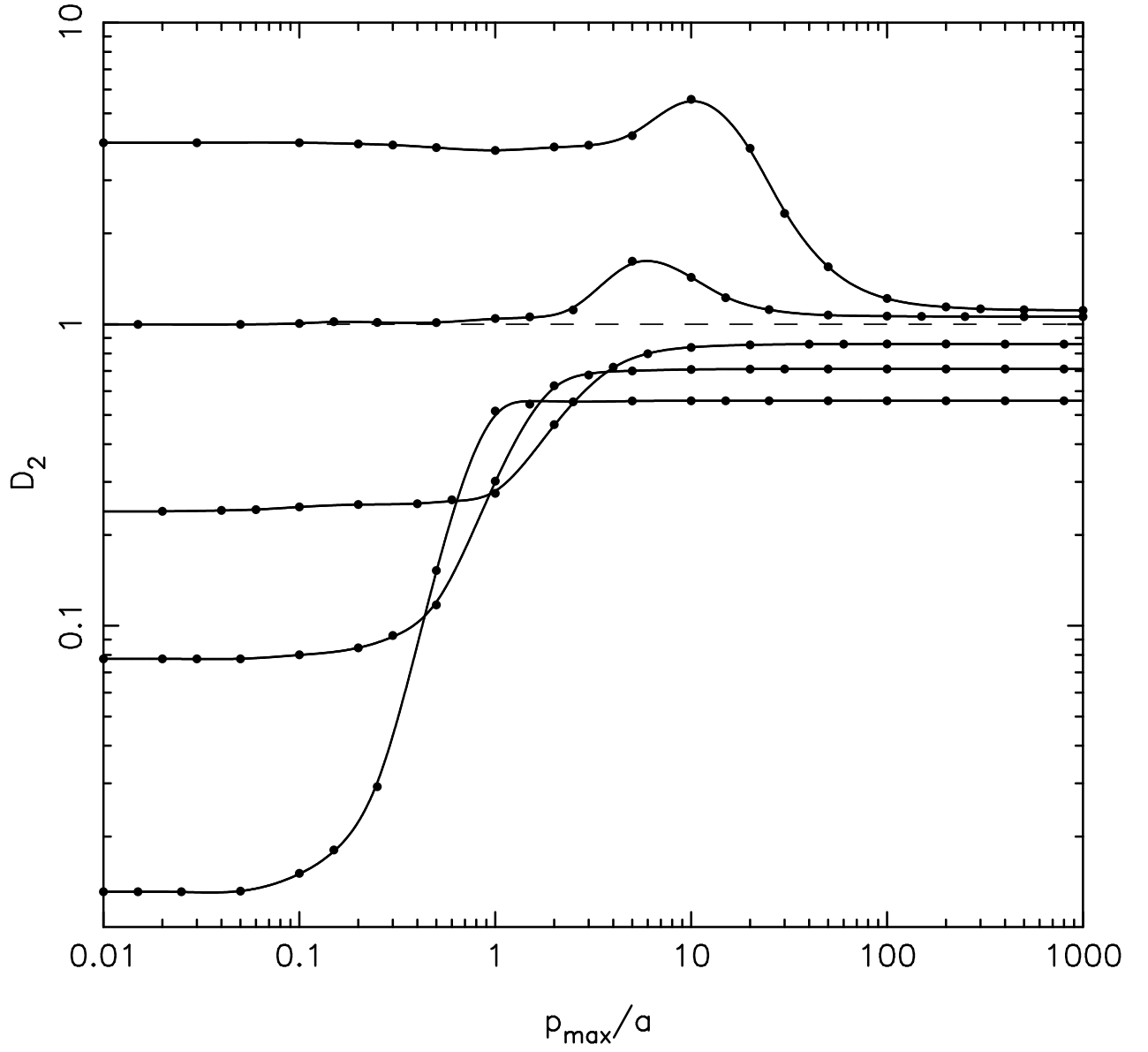


FIG. A8.— Dimensionless ratio $D_2(V, p_{\max})$ (eq. 72a) describing changes in the mean square field-star velocity in a direction parallel to the initial velocity, normalized to the value for a point-mass scatterer. Different curves correspond to $V/V_{\text{bin}} = (0.1, 0.2, 0.5, 1, 2)$; the lowest (highest) V produces the highest (lowest) D_2 at small p_{\max} .

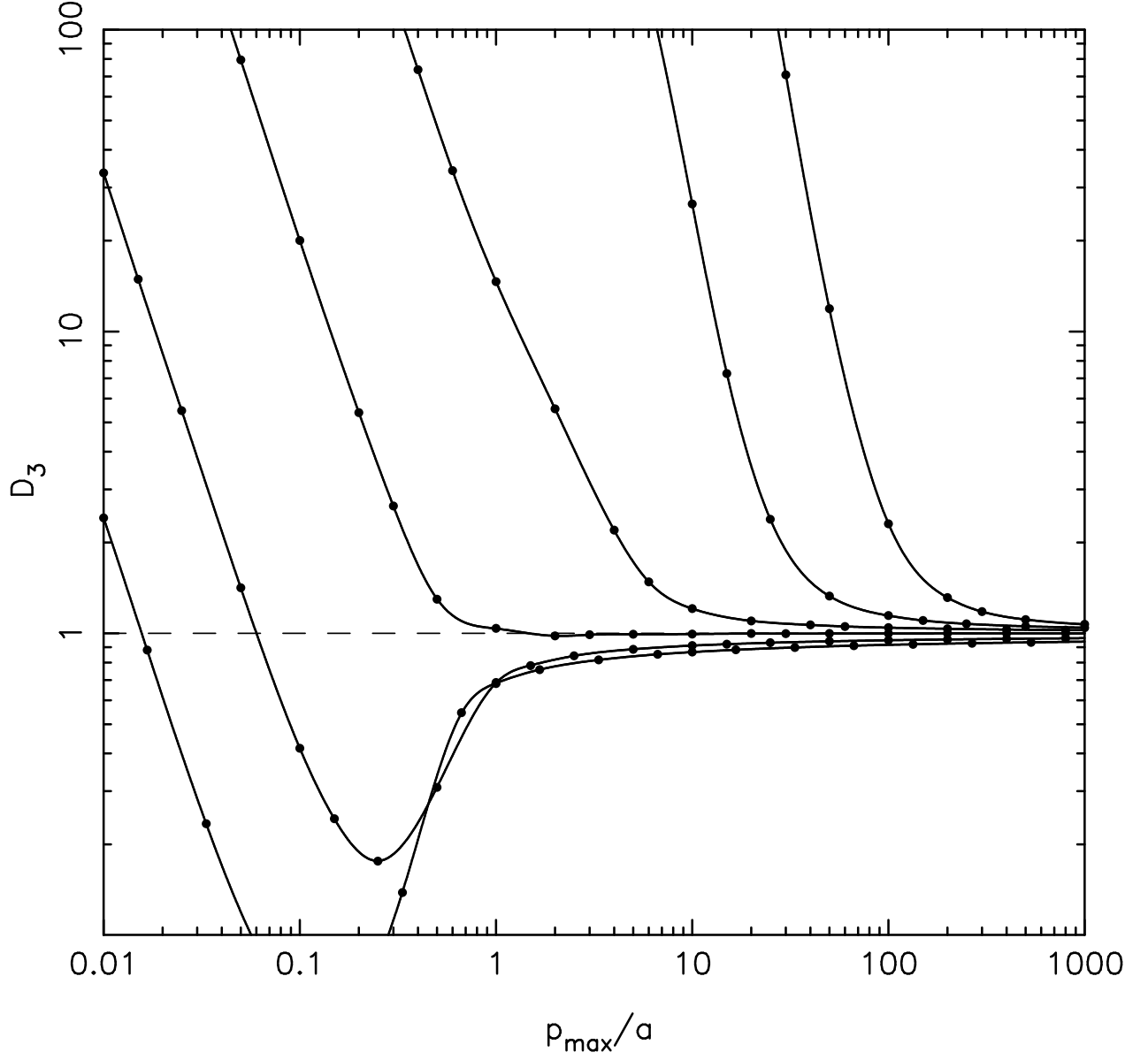


FIG. A9.— Dimensionless ratio $D_3(V, p_{max})$ (eq. 72b) describing changes in the mean square field-star velocity in a direction perpendicular to the initial velocity, normalized to the value for a point-mass scatterer. Different curves correspond to $V/V_{bin} = 0.1, 0.2, 0.5, 1, 2, 3$; the lowest (highest) V produces the highest (lowest) D_3 at small p_{max} .

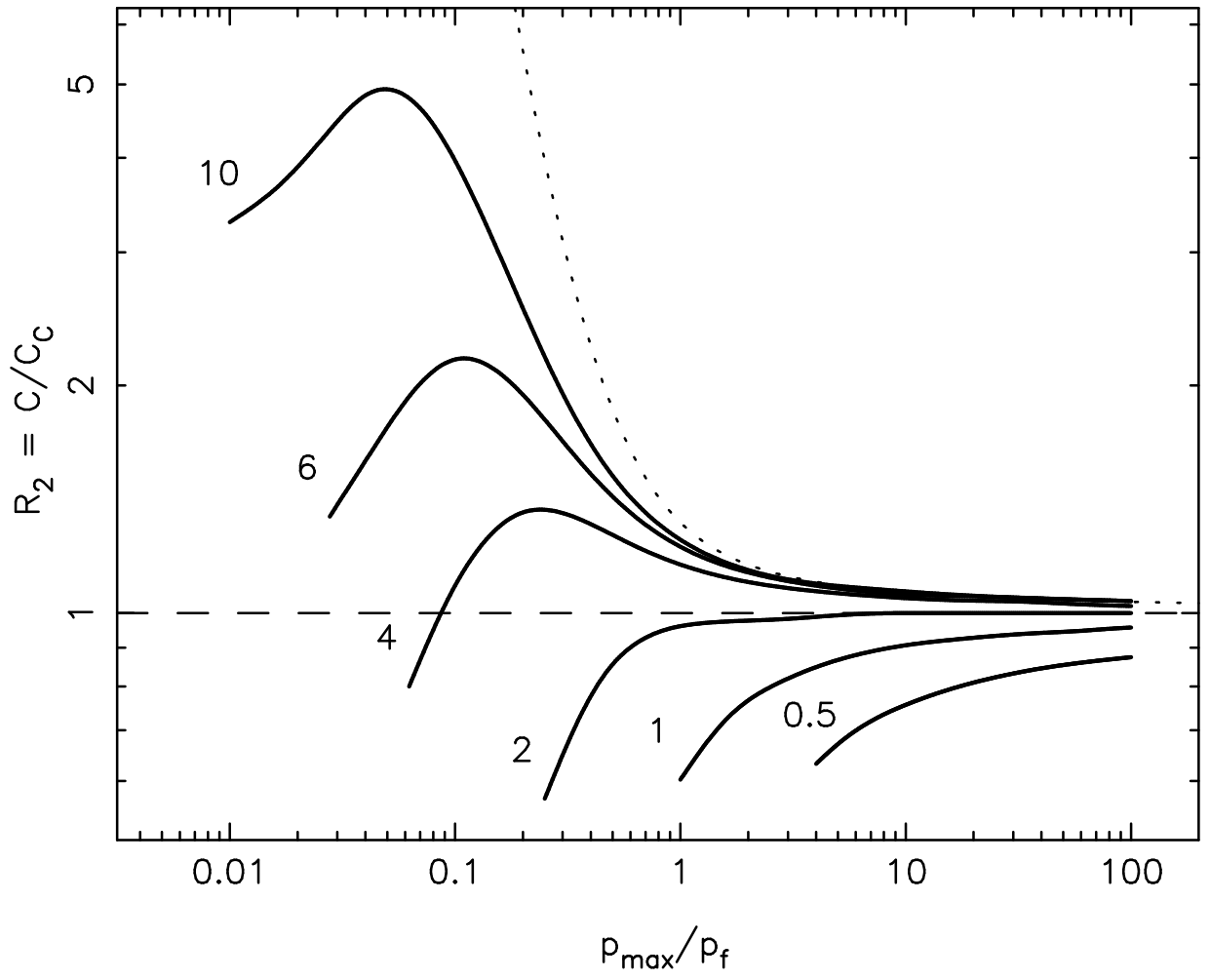


FIG. A10.— Increase in the diffusion coefficient $\langle \Delta v^2 \rangle$ for a massive binary moving at low velocity, $v \ll \sigma_f$, compared to its value for a point mass. Curves are labelled by the value of V_{bin}/σ_f . Dashed line is the approximation of equation (74).

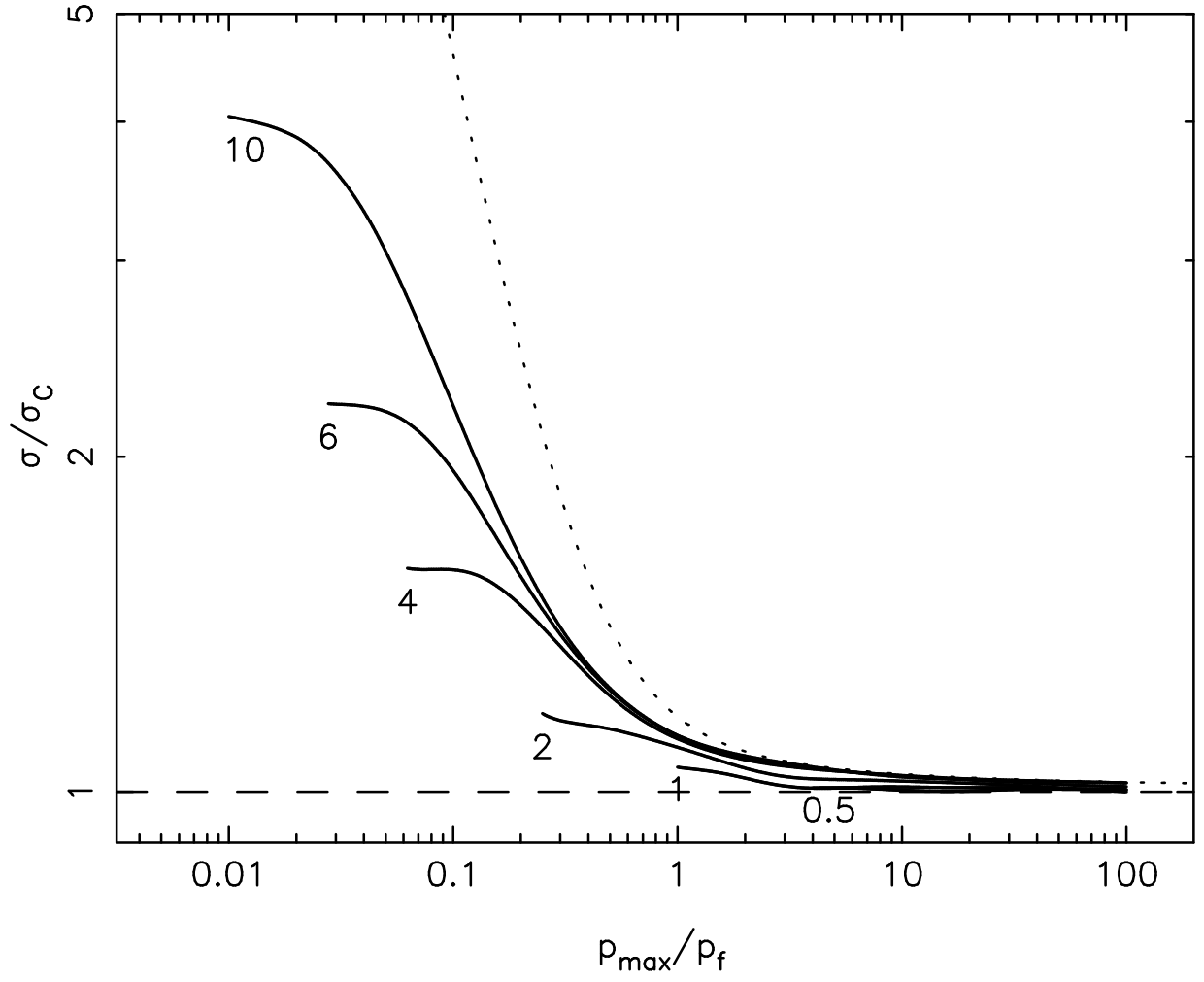


FIG. A11.— Increase in the equilibrium velocity dispersion of a massive binary compared to its value for a point mass. Curves are labelled by the value of V_{bin}/σ_f . Dashed line is the approximation of equation (75).